ECHOES OF BERT: DO MODERN LANGUAGE MODELS REDISCOVER THE CLASSICAL NLP PIPELINE?

Anonymous authors
Paper under double-blind review

ABSTRACT

Large transformer-based language models dominate modern NLP, yet our understanding of how they encode linguistic information relies primarily on studies of early models like `BERT` and `GPT-2`. Building on prior BERTology work, we analyze 25 models spanning classical architectures (`BERT`, `DeBERTa`, `GPT-2`) to modern large language models (`Pythia`, `OLMo-2`, `Gemma-2`, `Qwen2.5`, `Llama-3.1`), probing layer-by-layer representations across eight linguistic tasks in English. Consistent with earlier findings, we find that hierarchical organization persists in modern models: early layers capture syntax, middle layers handle semantics and entity-level information, and later layers encode discourse phenomena. However, larger models compress this entire hierarchy toward earlier layer positions, suggesting they build richer representations more quickly. We dive deeper, conducting an in-depth multilingual analysis of two linguistic properties - lemma identity and inflectional features - that help disentangle form from meaning. We find that lemma information concentrates linearly in early layers but becomes increasingly nonlinear deeper in the network, while inflectional information remains linearly accessible throughout all layers. Additional analyses of attention mechanisms, steering vectors, and pretraining checkpoints reveal where this information resides within layers, how it can be functionally manipulated, and how representations evolve during pretraining. Taken together, our findings suggest that, even with substantial advances in LLM technologies, transformer models learn to organize linguistic information in similar ways, regardless of model architecture, size, or training regime, indicating that these properties are important for next token prediction.

1 INTRODUCTION

Large transformer-based language models (LMs) are widely used for tasks such as text generation, question answering, and code completion (Workshop, 2023; Groeneveld et al., 2024; Llama, 2024; Hui et al., 2024) However, how these models internally represent linguistic information remains an active research area. Prior work suggests a hierarchical organization where different layers specialize in capturing distinct levels of linguistic structure, from surface features to syntax and semantics (Jawahar et al., 2019; Tenney et al., 2019a; Rogers et al., 2020).

But these studies focus only on first-generation LMs such as `BERT` and `GPT-2` (Devlin et al., 2019; Radford et al., 2019). Since then, language technology has transformed dramatically - today's models differ in architecture (encoder-only, decoder-only, encoder–decoder), pretraining objectives (masked vs. causal language modeling), training data volume (billions vs. trillions of tokens), and post-training adaptation. (Brown et al., 2020; Groeneveld et al., 2024; Lambert et al., 2025). We ask: do modern LMS *rediscover the classical NLP pipeline* observed in early models, and how does model scale and architecture influence where and how linguistic structure is encoded?

To answer these questions we systematically probe 25 pretrained models ranging from `BERT Base` to `Llama-3.1 8B`, spanning multiple architectures, sizes, and training regimes. We train simple classifiers at each layer to predict eight linguistic tasks in English and evaluate where information emerges.

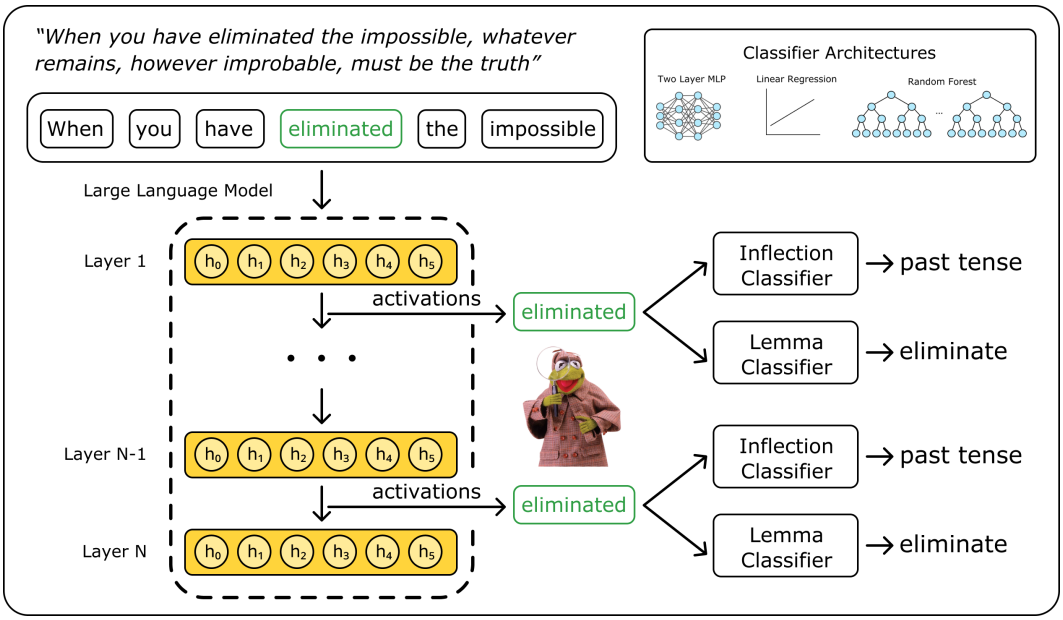

Figure 1: Overview of our probing methodology. We extract hidden state activations from each model layer for target words and train simple linear and shallow non-linear classifiers for token, span and pairwise edge predictions (POS, dependencies, constituents, NER, SRL, SPR, coreference, and relations), as well as word-level lemma and inflection prediction. We compute selectivity using control labels and summarize where performance emerges with expected layer and center of gravity.

Beyond this pipeline analysis, we perform a targeted case study on two linguistic properties: *lemma identity* and *inflectional features*. These properties help disentangle meaning from surface form - consider the words *walk*, *walked*, *jump*, and *jumped*. Do language models group words by shared meaning (*walk*, *walked*) or by shared grammar (*walked*, *jumped*)? More broadly, where and how do LMs encode a word's lemma and its inflectional features?

We examine six typologically diverse languages - English, Chinese, German, French, Russian, and Turkish - to test whether observed patterns generalize beyond English. We also test where lemma and inflectional information resides (attention heads vs. residual streams), track when these representations emerge during pretraining, and evaluate the impact of editing activations via steering vectors. We find that:

1. Modern LMs rediscover the classical NLP pipeline. Syntactic tasks peak earliest, semantic tasks peak in the middle, and discourse tasks peak latest. Larger models compress this pipeline towards shallower layers, suggesting they learn richer representations more quickly.
2. Lemma information is encoded prominently in early layers and becomes increasingly non-linear deeper in the network, whereas inflectional information remains linearly accessible across all layers and languages.
3. Lemma and inflectional information emerge early in pretraining and reside primarily in the residual stream; inflectional features occupy compact, steerable subspaces that enable effective interventions.

2 Probe Design and Metrics

We investigate how language models encode linguistic information using simple classifiers (*probes*) trained on activations from individual layers. Following Tenney et al. (2019b), we consider three types of predictions: token-level tasks (*e.g.*, , POS), span-level tasks (constituency, named entity recognition, semantic role labeling, semantic proto-roles), and edge or pairwise tasks (dependency arcs and coreference links). For our case study we additionally train probes to predict each word's lemma and its inflectional features.

2.1 PROBE ARCHITECTURES

For each layer of a model we extract residual-stream representations for a target word, span or pair and train two simple classifiers: a linear regression probe and non-linear multi-layer perceptron (MLP) probe. The linear probe measures how well information is linearly separable in the representation space, while the non-linear probe tests whether a non-linear decision boundary yields better performance. Comparing these probes allows us to infer whether a property is encoded *linearly* or *non-linearly*. Architecture details and hyperparameters are provided in Appendix C.

2.2 REPRESENTATIONS AND TASKS

For token-level tasks we use the representation of the last subword token for the target word; for span-level tasks we mean-pool representations across subwords; for pairwise tasks we concatenate and element-wise combine representations following Tenney et al. (2019b).

We evaluate eight linguistic tasks introduced by Tenney et al. (2019a), covering the classical NLP pipeline from syntax to discourse. At the syntactic level, we consider part-of-speech tagging, constituency parsing (phrase structure), and dependency parsing (head–dependent relations); at the semantic level, named entity recognition (persons, organizations, locations), semantic role labeling (agent and patient roles), and semantic proto-role labeling (*e.g.*, , volition, sentience); and at the discourse level, coreference resolution and relation extraction (relations between entities). Formal task definitions are provided in Appendix D.

2.3 METRICS

We define several metrics for localizing where information emerges with depth and for quantifying nonlinearity: selectivity, the linear separability gap, and two depth statistics inspired by Tenney et al. (2019a), expected layer and center of gravity.

Selectivity. Probes may simply memorize training data rather than extracting true linguistic information from the representations. To account for this, we train identical probes on randomly permuted labels (control tasks) following Hewitt & Liang (2019). We define selectivity at layer ℓ as the difference between real and control accuracies:

$$\text{Sel}_\ell = \text{Acc}_\ell^{\text{real}} - \text{Acc}_\ell^{\text{control}} \tag{1}$$

Higher values mean the classifier is extracting true linguistic information rather than memorizing.

Linear separability gap. We quantify nonlinearity at a layer as the difference in accuracy between a non-linear and linear probe:

$$\text{Gap}_\ell = \text{Acc}_\ell^{\text{nonlin}} - \text{Acc}_\ell^{\text{linear}}, \tag{2}$$

where positive values indicate useful information is present but not linearly separable.

Center of gravity and expected layer. Let a_ℓ be the test accuracy using layer ℓ for $\ell = 0, \ldots, L$, and let $b_\ell = \max_{j \le \ell} a_j$ be the cumulative (best-so-far) curve. We weight layers by their consolidation relative to the baseline and take an index-weighted average:

$$w_\ell = \frac{b_\ell - b_0}{\sum_{k=0}^{L}(b_k - b_0)}, \quad \text{CenterOfGravity} = \sum_{\ell=0}^{L} \ell \, w_\ell. \tag{3}$$

Then, to localize where marginal gains first occur, we use the nonnegative increments of the cumulative curve and take their weighted average:

$$\Delta_\ell = \max(b_\ell - b_{\ell-1}, 0)\,, \quad p_\ell = \frac{\Delta_\ell}{\sum_{j=1}^{L} \Delta_j}, \quad \text{ExpectedLayer} = \sum_{\ell=1}^{L} \ell \, p_\ell. \tag{4}$$

Unlike center of gravity (which weights consolidated performance), this emphasizes where useful information first becomes available, highlighting the specific layers at which the model begins to encode properties relevant to the task.

3 EXPERIMENTS

Using the methodology introduced in Section §2, we describe the components of our experimental setup: the datasets, model suite, and procedure for extracting token-level representations.

3.1 DATASETS

We use several annotated datasets for our eight classical NLP pipeline tasks: UD English-GUM (POS, dependencies, named entities, coreference, constituents) (Nivre et al., 2016; Zeldes, 2017), Universal Propositions English-EWT (SRL) (Jindal et al., 2022), SPR1 datasets (PropBank and UD-EWT sources; SPR), and SemEval-2010 Task 8 (relations). We use the same token/span/edge labeling schemes.

For our in-depth analysis of lemma identity and inflectional features, we use Universal Dependencies corpora across six languages - English, Chinese, German, French, Russian, Turkish (Nivre et al., 2016). We select GUM for English (Zeldes, 2017), GSD for Chinese/German/French (McDonald et al., 2013; Guillaume et al., 2019), SynTagRus for Russian (Droganova et al., 2018), and IMST for Turkish (Sulubacak et al., 2016). [1]

3.2 MODELS

We study a diverse set of pretrained transformer language models spanning different architectures, sizes, and training regimes. Table 1 lists all models used in this study (see Table 16 for the HuggingFace identifiers).

For English, we evaluate all models listed in Table 1 (excluding the non-English `Goldfish` models). For the five non-English languages (Chinese, German, French, Russian, Turkish), we focus on models that have explicit multilingual training: the `Goldfish` monolingual models trained specifically for each target language (Chang et al., 2024), multilingual `Qwen2.5` variants that include these languages in their training data, and the multilingual `mT5-base` model (Xue et al., 2021). This ensures that we evaluate models on languages they were trained on while maintaining sufficient coverage.

Table 1: Overview of models used in this study.

Model	Parameters	Pretraining Data	Layers
Encoder-only			
`BERT Base`	110M	12.6B tokens[1]	12
`BERT Large`	340M	12.6B tokens[1]	24
`DeBERTa V3 Large`	418M	32B tokens[1]	24
Decoder-only			
`GPT-2-Small`	124M	8B tokens[1]	12
`GPT-2-Large`	708M	8B tokens[1]	36
`GPT-2-XL`	1.5B	8B tokens[1]	48
`Goldfish English 1000mb`	124M	200M tokens	12
`Goldfish Chinese 1000mb`	124M	200M tokens	12
`Goldfish German 1000mb`	124M	200M tokens	12
`Goldfish French 1000mb`	124M	200M tokens	12
`Goldfish Russian 1000mb`	124M	200M tokens	12
`Goldfish Turkish 1000mb`	124M	200M tokens	12
`Pythia-6.9B`	6900M	300B tokens	32
`Pythia-6.9B Tulu`	6900M	300B tokens	32
`OLMo-2-7B`	7300M	4T tokens	32
`OLMo-2-7B-Instruct`	7300M	4T tokens	32
`Gemma-2-2B`	2610M	2T tokens	26
`Gemma-2-2B-Instruct`	2610M	2T tokens	26
`Qwen2.5-1.5B`	1540M	18T tokens	28
`Qwen2.5-1.5B-Instruct`	1540M	18T tokens	28
`Qwen2.5-7B`	7620M	18T tokens	28
`Qwen2.5-7B-Instruct`	7620M	18T tokens	28
`Llama-3.1-8B`	8000M	15T tokens	32
`Llama-3.1-8B-Instruct`	8000M	15T tokens	32
Encoder-Decoder			
`mT5-base`	580M	1T tokens	12

[1] Converted from GB to tokens using the approximation that 1GB of data is approximately 200M tokens in English (Chang et al., 2024).

3.3 REPRESENTATION EXTRACTION

We tokenize inputs with model-specific tokenizers and run a forward pass to collect residual-stream activations from every layer. Token, span, and pair encodings follow Section §2. For words split into multiple subwords, we use the last subword's representation (Devlin et al., 2019). Models are used as-is (no fine-tuning), and we report results by layer using these activations.

[1] See Appendix §H for complete details including dataset statistics, tokenization information, and visualizations for all languages

4 THE CLASSICAL NLP PIPELINE

We probe 18 models across eight linguistic tasks to test whether modern language models rediscover the classical NLP pipeline. In this section, we present three representative models - encoder-only, decoder-only and instruction-tuned architectures - with full results for all models in Appendix §E.

4.1 LAYERWISE PATTERNS CLEANLY SEPARATE MODEL FAMILIES

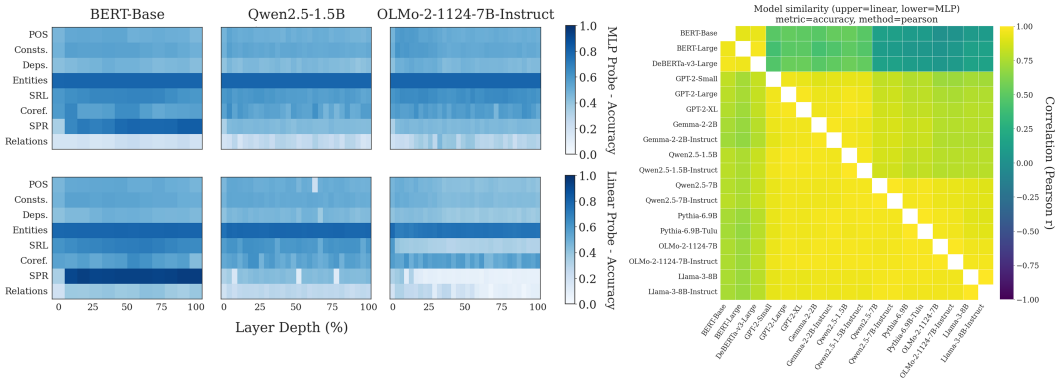

Figure 2: **Left:** Probe accuracy across layers for `BERT Base`, `Qwen2.5-1.5B`, and `OLMo-2-1124-7B-Instruct`. Top panels show MLP probes and bottom panel show linear probes. **Right:** Pearson correlations between all models, computed from flattening each model's task-by-layer accuracy grid and correlating across all pairs of models. Lower triangle: MLP correlations; upper triangle: linear correlations

Probe performance. Our results in Figure 2 (left) show that MLP probes consistently match or exceed linear probe accuracy across all tasks (see Figures 7 and 8 for complete results). The linear separability gap - the difference between MLP and linear performance - peaks for late-pipeline tasks, specifically SPR and Relations. This pattern holds across all 18 models (see Appendix §E).

Model correlations. The correlation matrix, Figure 2 (right), provides a global summary between all 18 models. A high correlation indicates that two models' layerwise accuracies across tasks are similar; low correlations indicate divergent accuracy patterns. We observe three distinct trends:

1. *Models cluster by architecture.* Encoder-only models (*e.g.*, `BERT` and `DeBERTa`) correlate strongly with each other while having low correlations with decoder models. The same is true for decoder-only architectures, such as `GPT-2`, `Pythia`, `Qwen2.5` and `Llama 3.1`, which form their own cluster with high internal similarity.
2. *Instruction tuning preserves base model latent structure.* Fine-tuned variants maintain high correlations with their base counterparts, indicating that post-training does not fundamentally reorganize linguistic representations.
3. *Model size forms a secondary clustering, but only for linear probes.* Models around one billion parameters group together separately from 7B+ models for linear probe accuracy. MLP probes don't show this size-based clustering, likely because their additional capacity masks any scale-dependent representation differences.

4.2 LARGER MODEL COMPRESS THE HIERARCHY

To pinpoint where linguistic properties emerge and consolidate, we compute compute expected layer and center of gravity as defined in Section 2. Intuitively, the *expected layer* captures marginal accuracy gains and highlights the depth at which information first emerges, while *center of gravity* weights each layer by cumulative best accuracy to locate performance ultimately consolidates most strongly.

The hierarchy persists. Figure 3 shows a shared relative ordering partially emerges across all models. Syntactic tasks (POS, Constituency, Dependencies) tend to emerge before semantic tasks

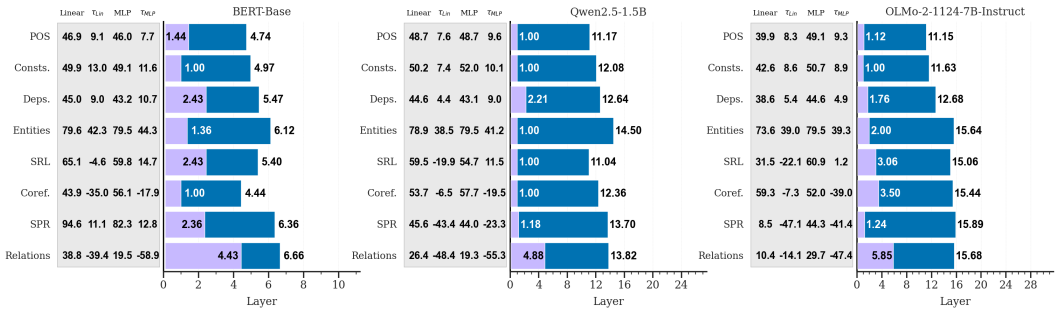

Figure 3: Expected layer (blue) and center of gravity (purple) for the same three models. The left four columns show accuracy and selectivity (τ) for linear and MLP probes, averaged across layers. Selectivity measures how much of the accuracy is due to genuine signal rather than memorization by the probe.

(Entities, SRL, SPR), which emerge before discourse phenomena (Corefernce, Relations). However, this hierarchical progression is less distinct in modern models than in early ones, suggesting that the hierarchy exists but is compressed.

Scale compresses depth. Model capacity determines *where* and *whether* this hierarchy forms. For example, `BERT Base` (12 layers) places relation extraction around layer 8, while both `Qwen2.5-1.5B` (28 layers) and `OLMo-2-7B-Instruct` (32 layers) compress it to approximately one-fifth depth. Larger models seem to encode the complete linguistic hierarchy using fewer layers, suggesting that they build useful representations earlier.

Selectivity reveals probe limitations. MLP probes appear to achieve high accuracy, but have strong negative selectivity, meaning they memorize the task rather than extract meaningful information from the representations. Linear probes are better, showing positive selectivity for syntactic tasks. However, they drop to near zero selectivity for discourse tasks (Coreference, Relations), suggesting that while discourse information exists in representations, linear decoding struggles to extract it cleanly.

4.3 Discussion

Our analysis establishes two key findings:

1. The hierarchical organization observed in early transformers survives in modern models but with less separation between levels. But this relative ordering is detectable across architectures (encoder, decoder, encoder–decoder), training regimes (causal and masked language modeling, instruction tuning), and scale (100M to 8B parameters), but boundaries blur as models compress the pipeline.
2. Modern models encode all linguistic levels at shallower depths. Where `BERT Base` clearly separated syntactic, semantic, and discourse processing across its layers, a 7B model (`OLMo-2-7B-Instruct`) compresses this entire hierarchy into its early layers. This compression is evidence that as models become more powerful, they need fewer layers to learn this hierarchical linguistic structure, perhaps because they have higher representational capacity per layer and benefit from more extensive training.

These results suggest that while the classical NLP pipeline represented how early transformers organized knowledge, modern models develop a more compressed, interleaved representation of linguistic structure.

5 Lemma Identity and Inflectional Features

We now examine two important token-level properties: lemma identity and inflectional features. Using the same probing framework from Section §4, we expand to six typologically diverse languages: English, Chinese, German, French, Russian, and Turkish. We investigate where these properties emerge in model representations and how they become linearly accessible across layers.

5.1 RESULTS

We report layer-wise accuracies for lemma and inflection prediction across classifier types and languages. We evaluate 19 English models and six multi/monolingual models across lemma and inflection prediction tasks. Detailed layer-wise accuracy and selectivity tables are provided in Appendix §G.

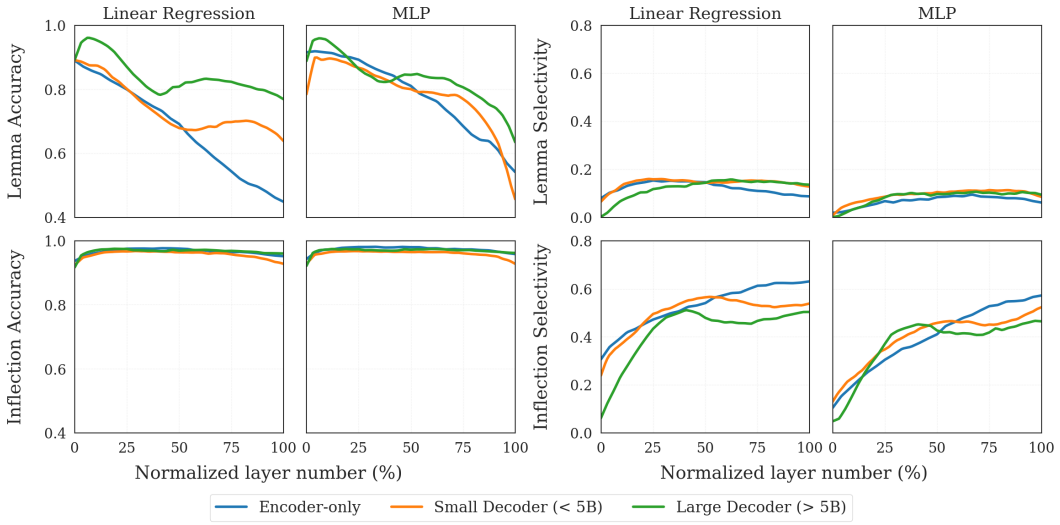

Figure 4: Lemma and inflection probing results for English, *averaged by model category*: encoder-only (`BERT`, `DeBERTa`), small decoder <5B (`GPT-2`, `Gemma-2-2B` (and instruct), `Qwen2.5-1.5B` (and instruct)), and large decoder >5B (`Pythia-6.9B`, `OLMo-2-7B`, `Llama-3.1-8B` and instruct versions). Columns show prediction accuracy (Linear vs. MLP probes) and selectivity scores (linguistic minus control accuracy). Note that for readability, the y-axis for accuracy starts at 0.4. Full (non-averaged) results for individual models are provided in Appendix §F.

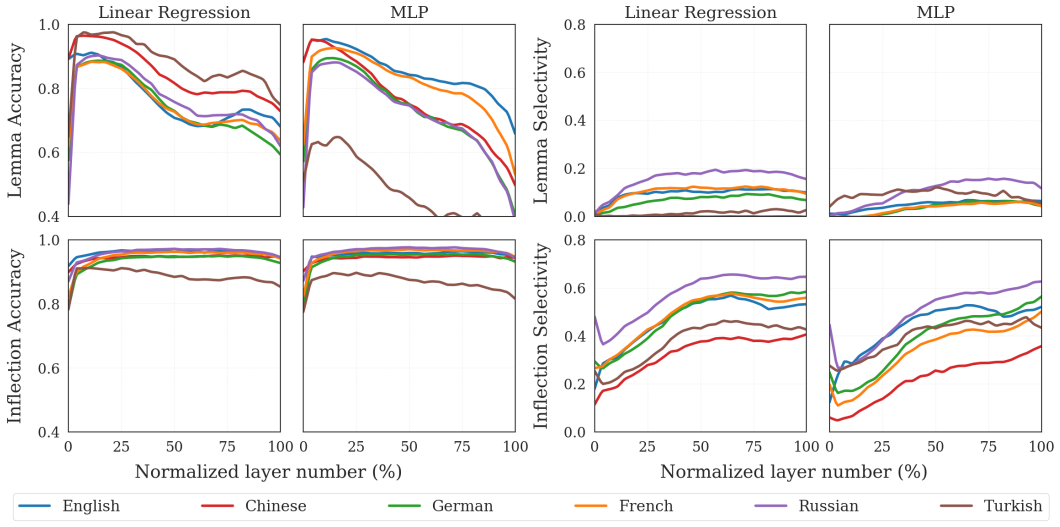

Figure 5: Cross-linguistic probing results *averaged across all models within each language*. Each language averages over multilingual models `mT5-base`, `Qwen2.5-1.5B` (and instruct), `Qwen2.5-7B` (and instruct) and its corresponding monolingual `Goldfish <Language> 1000mb` model (*e.g.*, `Goldfish English 1000mb`). Columns show lemma and inflection accuracy (Linear vs. MLP) followed by selectivity scores. Note that for readability, the y-axis for accuracy starts at 0.4. Full (non-averaged) results for individual models are provided in Appendix §F.

Lemma. Lemma accuracy under linear regression starts high (0.8–1.0) and decreases with depth in all English model families (Figure 4, top left). Encoder-only models show the strongest decrease, while small decoders decline more gradually and large decoders maintain higher accuracy in deeper layers. Across languages (Figure 5, top left), Turkish shows the largest drop (0.95 to 0.25), while Russian and Chinese retain 0.6–0.8 accuracy in later layers. MLP accuracy is similar but slightly higher than linear at most depths (middle column). Selectivity for lemma remains close to zero across depths and languages (right column), indicating that high lemma accuracy early in the network is mostly driven by surface correlations rather than strongly selective lexical structure.

Inflection. Inflectional features remain readable across all layers and architectures. For English, linear regression accuracy stays near 0.9–1.0 throughout the layers (Figure 4, bottom left). This pattern holds cross-linguistically (Figure 5, bottom left): English, German, French, and Russian exceed 0.9 accuracy at most depths, while Turkish is slightly lower, hovering around 0.8–0.9. MLP probes follow the same pattern (middle column). Selectivity scores for inflection remain positive (0.4–0.6) across models and languages (right column), with Russian and German at the upper end, supporting the view that inflectional features are encoded in stable, linearly accessible subspaces.

Probe error analysis. Frequency strongly correlates with probe accuracy for both tasks. Frequent lemmas and inflectional categories achieve higher accuracy, while rare words and rare inflections account for most errors. For inflection, comparative and superlative degrees and low-frequency verb forms are the most error-prone categories. Turkish shows the strongest sensitivity to frequency, likely due to its morphological complexity creating a long tail of rare forms. A detailed breakdown by part of speech and inflectional category is given in Appendix §L.

5.2 Analysis

Our results show that lemma identity is encoded strongly in early layers but becomes less accessible in deeper layers, whereas inflectional features remain robustly decodable throughout the model. We analyze this further along several axes.

Inflection is linearly separable; lemma shows limited nonlinearity. We report the linear separability gap, defined in equation (2), which measures the accuracy difference between MLP and linear probes. Detailed plots for lemma and inflection appear in Appendix §I.3. For inflection, the gap stays close to zero across layers, architectures, and languages, typically within ± 0.02 accuracy, consistent with the near-overlap of linear and MLP curves in Figures 4 and 5. This is evidence that inflectional features are encoded linearly in the representations. For lemma, gaps are modest but positive, especially in early and middle layers of encoder-only models and smaller decoders, where MLPs achieve slightly higher accuracy than linear probes before both degrade in deeper layers. This suggests that lemma information is present but less linearly separable than inflection.

Some models show extreme mid-layer dimensionality compression; others gradually compress representations. To characterize the representation geometry of these models, we estimate intrinsic dimensionality by counting the fraction of principal components required to reach fixed variance thresholds over our entire dataset of collected activations (full results appear in Appendix §I.1).Encoder-only models (`BERT`, `DeBERTa`) and several decoders (`Gemma`, `Llama`, `OLMo-2`) exhibit gradual compression: even at 90–99% variance, the relative number of components decreases only slowly as depth increases. In contrast, `GPT-2`, `Qwen2.5`, and `Pythia` enter a regime in their middle layers where very few components - often just a single dimension - account for most of the variance at these thresholds. Analysis of activation statistics (Appendix §I.2) reveals that this low intrinsic dimensionality is driven by outlier dimensions with large activation values: models like `Qwen2.5-1.5B` reach maximum absolute activations of 8000 in middle layers, while models like `Llama-3-8B` reach values of only 30-40 (Sun et al., 2024; Rudman et al., 2023).

Residual streams retain more linguistic information than attention outputs. Probing attention-head outputs and residual-stream activations for `BERT` and contemporary decoders (Figures 27 and 28) highlights different roles for these components. For both lemma and inflection, probes on attention outputs yield lower accuracy than probes on the residual stream at almost all depths. For lemma, attention-based accuracy falls to around 0.2–0.4 in middle layers, while residual streams remain closer to 0.6–0.9. For inflection, both components maintain high accuracy (0.7–1.0), but residual streams consistently outperform attention outputs, particularly in middle layers. Selectivity follows the same pattern: lemma selectivity is near zero for attention outputs and higher for residuals, while

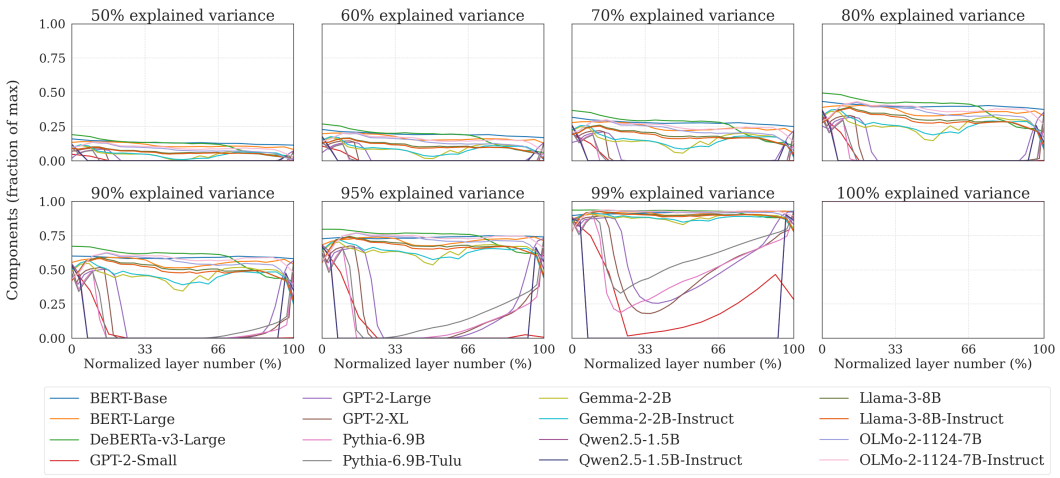

Figure 6: Intrinsic dimensionality across layers. Lines show fraction of PCA components needed to reach variance thresholds (50–100%). Models with strong mid-layer compression (few components for high variance) align with the inflection-is-linear, lemma-is-nonlinear split. Full curves per model appear in Figure 15.

inflection selectivity reaches 0.4–0.5 in both streams with residuals slightly higher. These results support a view in which attention primarily aggregates contextual relationships, whereas the residual stream/MLP layers preserve token-level lexical and morphological information that supports both lemma and inflection prediction.

Inflection steering effectiveness tracks intrinsic dimensionality. Steering experiments with inflection features (*e.g.*, , singular vs. plural) connect these representational properties to causal control. For each pair of categories, we compute a difference vector between mean hidden states and apply scaled interventions at each layer. Figures 29 and 30 show that, for most architectures and layers, even moderate steering scales (*e.g.*, , $\lambda = 5$) yield large changes in predicted inflection and high flip rates, indicating that a single direction in activation space can reliably control morphological representations. `Qwen2.5` variants demonstrate an interesting property: in their early–middle layers, steering is much less effective, with both probability change and flip rate reaching their minima. This region aligns with the layers where intrinsic dimensionality is lowest in Figures 6 and 15. Combined with the accuracy curves in Figure 4, this suggests that strongly compressed representations are more resistant to causal manipulation, even when inflection remains linearly decodable, whereas higher-dimensional layers permit more effective steering of inflectional morphology.

Inflection stabilizes early in training; lemma continues to change. Pretraining checkpoint analysis for `OLMo-2-7B` and `Pythia-6.9B` (Figures 25 and 26) shows that morphological analysis emerges very early, whereas lemma information continues to evolve with training. For both model families, inflection accuracy is already high at the earliest checkpoints and increases only slightly with additional updates; inflection selectivity grows quickly in the first few checkpoints and then remains near its final value. Lemma behaves differently. In `OLMo-2-7B`, lemma accuracy and selectivity increase gradually across checkpoints, with the largest gains in middle layers. In `Pythia-6.9B`, early checkpoints exhibit much lower lemma accuracy and near-zero lemma selectivity in deeper layers, and both quantities rise steadily as training progresses. These trends indicate that models identify and stabilize inflectional categories early in pretraining, while lemma representations remain more plastic and continue to be reshaped throughout training, especially in the later layers of decoder-only models.

5.3 Discussion

The previous analyses present a comprehensive picture of how lemma identity and inflectional features are organized inside transformer language models. Lemma information is strongly encoded in early layers but becomes less accessible as depth increases, particularly in models that undergo strong mid-layer compression. Inflectional features, in contrast, remain decodable across virtually all layers and models, with small linear separability gaps and high selectivity.

The linear separability results suggest that grammatical features are encoded in low-dimensional, approximately linear subspaces, while lemma identity relies more on higher-variance directions that are later deemphasized. Intrinsic dimensionality measurements, together with the steering experiments, tell us that aggressive compression in some decoder-only models limits the space in which such directions can be causally manipulated. Specifically, steering remains effective in higher-dimensional regions but degrades in layers whose variance is captured by very few components. The comparison between attention outputs and residual streams further implies that lexical information is preserved in the residual stream.

Taken together, these findings point to an organization in which inflection is a stable and linearly accessible component of the internal state, supporting both probing and controlled interventions, while lemma identity is encoded in a way that is useful for early processing but increasingly traded off against compact, context-oriented representations as models optimize for next-token prediction.

6 Related Work

Probing for linguistic information. Probing studies typically use supervised classifiers to predict linguistic properties from model representations (Alain & Bengio, 2017; Adi et al., 2017). Extensive work has established that early transformer models (`BERT`, `GPT-2`) learn hierarchical linguistic structures, with different layers specializing in different information types: lower layers capture surface features and morphology, middle layers encode syntax, and upper layers represent semantics and context (Jawahar et al., 2019; Tenney et al., 2019a; Rogers et al., 2020). More relevant to our work, Vulić et al. (2020) found that lexical information concentrates in lower layers, while Ethayarajh (2019) showed that representations become increasingly context-specific in higher layers.

Representation dynamics in modern LLMs. Recent research has extended these analyses to modern, larger-scale generative models, examining how representational geometry evolves with scale. Cheng et al. (2025) identify a distinct high-dimensional abstraction phase in the early-to-middle layers of models like Llama and OLMo, suggesting that the transition from surface-level to abstract linguistic features occurs earlier than in previous architectures. Similarly, Skean et al. (2025) demonstrate that intermediate layers in modern LLMs often encode richer task-transferable representations than final layers, challenging the assumption that semantic capability monotonically increases with depth. These findings align with the pipeline compression we observe in Section §3.

Activation steering. Beyond probing, recent work has explored manipulating model behavior by intervening on internal representations. This includes steering vectors (Subramani et al., 2022), inference-time interventions (Li et al., 2023), representation editing (Meng et al., 2022), sparse autoencoders for feature discovery (Bricken et al., 2023), and causal mediation analysis (Vig et al., 2020). While these methods typically evaluate changes in model outputs, our steering experiments focus on measuring representational changes. See Appendix §B for more detailed discussion.

Mechanistic interpretability and feature discovery. Mechanistic interpretability approaches aim to reverse-engineer the algorithms learned by neural networks (Elhage et al., 2021), offering a more causal view of internal structure. Recent work uses sparse autoencoders to decompose dense representations into interpretable latent features (Cunningham et al., 2023; Bricken et al., 2023), providing clearer targets for interpretation than raw activations. While probing detects correlations between representations and linguistic concepts, these methods seek to identify the specific components and causal circuits that implement these behaviors.

7 Conclusion

In this work, we analyzed 25 transformer models and found that modern LMs show signs of rediscovering the classical NLP pipeline, progressing from syntax to semantics and discourse. However, we observe that larger models compress this hierarchy into earlier layers, suggesting that increased capacity allows useful representations to emerge sooner. Our case study further reveals that while lemma identity becomes increasingly non-linear with depth, inflectional features remain linearly accessible and steerable within the residual stream across languages. Collectively, these findings indicate that despite rapid advances in scale and training, transformers converge on robust, shared mechanisms for organizing linguistic information.

8 Reproducibility Statement

We will release a GitHub repository containing code to reproduce dataset construction, probing experiments, and all plots and analyses. The main paper specifies the probe design and metrics (Section §2), datasets and model suite (Sections §3 and Table 1), and evaluation summaries for the classical pipeline and for lemma identity and inflectional features (Sections §4 and §5). The appendix provides complete classifier and training details, dataset statistics, and full-resolution figure grids referenced in the text. Together, these materials are intended to enable end-to-end reproduction of our results.

References

Yossi Adi, Einat Kermany, Yonatan Belinkov, Ofer Lavi, and Yoav Goldberg. Fine-grained analysis of sentence embeddings using auxiliary prediction tasks. In *5th International Conference on Learning Representations (Conference Track)*, 2017. URL https://openreview.net/forum?id=BJh6Ztuxl.

Guillaume Alain and Yoshua Bengio. Understanding intermediate layers using linear classifier probes. In *5th International Conference on Learning Representations (Workshop Track)*, 2017. URL https://openreview.net/forum?id=ryF7rTqgl.

Trenton Bricken, Adly Templeton, Joshua Batson, Brian Chen, Adam Jermyn, Tom Conerly, Nick Turner, Cem Anil, Carson Denison, Amanda Askell, Robert Lasenby, Yifan Wu, Shauna Kravec, Nicholas Schiefer, Tim Maxwell, Nicholas Joseph, Zac Hatfield-Dodds, Alex Tamkin, Karina Nguyen, Brayden McLean, Josiah E Burke, Tristan Hume, Shan Carter, Tom Henighan, and Christopher Olah. Towards monosemanticity: Decomposing language models with dictionary learning. *Transformer Circuits Thread*, 2023. https://transformer-circuits.pub/2023/monosemantic-features/index.html.

Tom B. Brown, Benjamin Mann, Nick Ryder, Melanie Subbiah, Jared Kaplan, Prafulla Dhariwal, Arvind Neelakantan, Pranav Shyam, Girish Sastry, Amanda Askell, Sandhini Agarwal, Ariel Herbert-Voss, Gretchen Krueger, Tom Henighan, Rewon Child, Aditya Ramesh, Daniel M. Ziegler, Jeffrey Wu, Clemens Winter, Christopher Hesse, Mark Chen, Eric Sigler, Mateusz Litwin, Scott Gray, Benjamin Chess, Jack Clark, Christopher Berner, Sam McCandlish, Alec Radford, Ilya Sutskever, and Dario Amodei. Language models are few-shot learners, 2020. URL https://arxiv.org/abs/2005.14165.

Tyler A. Chang, Catherine Arnett, Zhuowen Tu, and Benjamin K. Bergen. Goldfish: Monolingual language models for 350 languages, 2024. URL https://arxiv.org/abs/2408.10441.

Emily Cheng, Diego Doimo, Corentin Kervadec, Iuri Macocco, Lei Yu, Alessandro Laio, and Marco Baroni. Emergence of a high-dimensional abstraction phase in language transformers. In *The Thirteenth International Conference on Learning Representations*, 2025. URL https://openreview.net/forum?id=0fD3iIBhlV.

Hoagy Cunningham, Aidan Ewart, Logan Riggs, Robert Huben, and Lee Sharkey. Sparse autoencoders find highly interpretable features in language models, 2023. URL https://arxiv.org/abs/2309.08600.

Thao Anh Dang, Limor Raviv, and Lukas Galke. Tokenization and morphology in multilingual language models: A comparative analysis of mt5 and byt5, 2024. URL https://arxiv.org/abs/2410.11627.

Jacob Devlin, Ming-Wei Chang, Kenton Lee, and Kristina Toutanova. BERT: Pre-training of deep bidirectional transformers for language understanding. In Jill Burstein, Christy Doran, and Thamar Solorio (eds.), *Proceedings of the 2019 Conference of the North American Chapter of the Association for Computational Linguistics: Human Language Technologies, Volume 1 (Long and Short Papers)*, pp. 4171–4186, Minneapolis, Minnesota, June 2019. Association for Computational Linguistics. doi: 10.18653/v1/N19-1423. URL https://aclanthology.org/N19-1423/.

Kira Droganova, Olga Lyashevskaya, and Daniel Zeman. Data conversion and consistency of monolingual corpora: Russian ud treebanks. In *Proceedings of the 17th international workshop on treebanks and linguistic theories (tlt 2018)*, volume 155, pp. 53–66. Linköping University Electronic Press Linköping, Sweden, 2018.

Yanai Elazar, Shauli Ravfogel, Alon Jacovi, and Yoav Goldberg. Amnesic probing: Behavioral explanation with amnesic counterfactuals. *Transactions of the Association for Computational Linguistics*, 9:160–175, 2021. doi: 10.1162/tacl_a_00359. URL https://aclanthology.org/2021.tacl-1.10/.

Nelson Elhage, Neel Nanda, Catherine Olsson, Tom Henighan, Nicholas Joseph, Ben Mann, Amanda Askell, Yuntao Bai, Anna Chen, Tom Conerly, Nova DasSarma, Dawn Drain, Deep Ganguli, Zac Hatfield-Dodds, Danny Hernandez, Andy Jones, Jackson Kernion, Liane Lovitt, Kamal Ndousse, Dario Amodei, Tom Brown, Jack Clark, Jared Kaplan, Sam McCandlish, and Chris Olah. A mathematical framework for transformer circuits. *Transformer Circuits Thread*, 2021. https://transformer-circuits.pub/2021/framework/index.html.

Kawin Ethayarajh. How contextual are contextualized word representations? Comparing the geometry of BERT, ELMo, and GPT-2 embeddings. In Kentaro Inui, Jing Jiang, Vincent Ng, and Xiaojun Wan (eds.), *Proceedings of the 2019 Conference on Empirical Methods in Natural Language Processing and the 9th International Joint Conference on Natural Language Processing (EMNLP-IJCNLP)*, pp. 55–65, Hong Kong, China, November 2019. Association for Computational Linguistics. doi: 10.18653/v1/D19-1006. URL https://aclanthology.org/D19-1006/.

Atticus Geiger, Hanson Lu, Thomas F Icard, and Christopher Potts. Causal abstractions of neural networks. In A. Beygelzimer, Y. Dauphin, P. Liang, and J. Wortman Vaughan (eds.), *Advances in Neural Information Processing Systems*, 2021. URL https://openreview.net/forum?id=RmuXDtjDhG.

Daniel Gildea and Daniel Jurafsky. Automatic labeling of semantic roles. *Computational Linguistics*, 28(3):245–288, 2002. doi: 10.1162/089120102760275983. URL https://aclanthology.org/J02-3001/.

Dirk Groeneveld, Iz Beltagy, Evan Walsh, Akshita Bhagia, Rodney Kinney, Oyvind Tafjord, Ananya Jha, Hamish Ivison, Ian Magnusson, Yizhong Wang, Shane Arora, David Atkinson, Russell Authur, Khyathi Chandu, Arman Cohan, Jennifer Dumas, Yanai Elazar, Yuling Gu, Jack Hessel, Tushar Khot, William Merrill, Jacob Morrison, Niklas Muennighoff, Aakanksha Naik, Crystal Nam, Matthew Peters, Valentina Pyatkin, Abhilasha Ravichander, Dustin Schwenk, Saurabh Shah, William Smith, Emma Strubell, Nishant Subramani, Mitchell Wortsman, Pradeep Dasigi, Nathan Lambert, Kyle Richardson, Luke Zettlemoyer, Jesse Dodge, Kyle Lo, Luca Soldaini, Noah Smith, and Hannaneh Hajishirzi. OLMo: Accelerating the science of language models. In Lun-Wei Ku, Andre Martins, and Vivek Srikumar (eds.), *Proceedings of the 62nd Annual Meeting of the Association for Computational Linguistics (Volume 1: Long Papers)*, pp. 15789–15809, Bangkok, Thailand, August 2024. Association for Computational Linguistics. doi: 10.18653/v1/2024.acl-long.841. URL https://aclanthology.org/2024.acl-long.841/.

Bruno Guillaume, Marie-Catherine de Marneffe, and Guy Perrier. Conversion et améliorations de corpus du français annotés en Universal Dependencies [conversion and improvement of Universal Dependencies French corpora]. *Traitement Automatique des Langues*, 60(2):71–95, 2019. URL https://aclanthology.org/2019.tal-2.4/.

Iris Hendrickx, Su Nam Kim, Zornitsa Kozareva, Preslav Nakov, Diarmuid Ó Séaghdha, Sebastian Padó, Marco Pennacchiotti, Lorenza Romano, and Stan Szpakowicz. SemEval-2010 task 8: Multi-way classification of semantic relations between pairs of nominals. In Katrin Erk and Carlo Strapparava (eds.), *Proceedings of the 5th International Workshop on Semantic Evaluation*, pp. 33–38, Uppsala, Sweden, July 2010. Association for Computational Linguistics. URL https://aclanthology.org/S10-1006/.

John Hewitt and Percy Liang. Designing and interpreting probes with control tasks. In Kentaro Inui, Jing Jiang, Vincent Ng, and Xiaojun Wan (eds.), *Proceedings of the 2019 Conference on Empirical Methods in Natural Language Processing and the 9th International Joint Conference on*

Natural Language Processing (EMNLP-IJCNLP), pp. 2733–2743, Hong Kong, China, November 2019. Association for Computational Linguistics. doi: 10.18653/v1/D19-1275. URL https://aclanthology.org/D19-1275/.

Kurt Hornik, Maxwell Stinchcombe, and Halbert White. Multilayer feedforward networks are universal approximators. *Neural Networks*, 2(5):359–366, 1989. ISSN 0893-6080. doi: https://doi.org/10.1016/0893-6080(89)90020-8. URL https://www.sciencedirect.com/science/article/pii/0893608089900208.

Binyuan Hui, Jian Yang, Zeyu Cui, Jiaxi Yang, Dayiheng Liu, Lei Zhang, Tianyu Liu, Jiajun Zhang, Bowen Yu, Kai Dang, et al. Qwen2. 5-coder technical report. *arXiv preprint arXiv:2409.12186*, 2024.

Gabriel Ilharco, Marco Tulio Ribeiro, Mitchell Wortsman, Ludwig Schmidt, Hannaneh Hajishirzi, and Ali Farhadi. Editing models with task arithmetic. In *The Eleventh International Conference on Learning Representations*, 2023. URL https://openreview.net/forum?id=6t0Kwf8-jrj.

Ganesh Jawahar, Benoît Sagot, and Djamé Seddah. What does BERT learn about the structure of language? In Anna Korhonen, David Traum, and Lluís Màrquez (eds.), *Proceedings of the 57th Annual Meeting of the Association for Computational Linguistics*, pp. 3651–3657, Florence, Italy, July 2019. Association for Computational Linguistics. doi: 10.18653/v1/P19-1356. URL https://aclanthology.org/P19-1356/.

Ishan Jindal, Alexandre Rademaker, Michał Ulewicz, Ha Linh, Huyen Nguyen, Khoi-Nguyen Tran, Huaiyu Zhu, and Yunyao Li. Universal Proposition Bank 2.0. In Nicoletta Calzolari, Frédéric Béchet, Philippe Blache, Khalid Choukri, Christopher Cieri, Thierry Declerck, Sara Goggi, Hitoshi Isahara, Bente Maegaard, Joseph Mariani, Hélène Mazo, Jan Odijk, and Stelios Piperidis (eds.), *Proceedings of the Thirteenth Language Resources and Evaluation Conference*, pp. 1700–1711, Marseille, France, June 2022. European Language Resources Association. URL https://aclanthology.org/2022.lrec-1.181/.

Nathan Lambert, Jacob Morrison, Valentina Pyatkin, Shengyi Huang, Hamish Ivison, Faeze Brahman, Lester James V. Miranda, Alisa Liu, Nouha Dziri, Shane Lyu, Yuling Gu, Saumya Malik, Victoria Graf, Jena D. Hwang, Jiangjiang Yang, Ronan Le Bras, Oyvind Tafjord, Chris Wilhelm, Luca Soldaini, Noah A. Smith, Yizhong Wang, Pradeep Dasigi, and Hannaneh Hajishirzi. Tulu 3: Pushing frontiers in open language model post-training, 2025. URL https://arxiv.org/abs/2411.15124.

Kenneth Li, Oam Patel, Fernanda Viégas, Hanspeter Pfister, and Martin Wattenberg. Inference-time intervention: Eliciting truthful answers from a language model. In *Thirty-seventh Conference on Neural Information Processing Systems*, 2023. URL https://openreview.net/forum?id=aLLuYpn83y.

Nelson F. Liu, Matt Gardner, Yonatan Belinkov, Matthew E. Peters, and Noah A. Smith. Linguistic knowledge and transferability of contextual representations. In Jill Burstein, Christy Doran, and Thamar Solorio (eds.), *Proceedings of the 2019 Conference of the North American Chapter of the Association for Computational Linguistics: Human Language Technologies, Volume 1 (Long and Short Papers)*, pp. 1073–1094, Minneapolis, Minnesota, June 2019. Association for Computational Linguistics. doi: 10.18653/v1/N19-1112. URL https://aclanthology.org/N19-1112/.

Team Llama. The llama 3 herd of models, 2024. URL https://arxiv.org/abs/2407.21783.

Mitchell P. Marcus, Beatrice Santorini, and Mary Ann Marcinkiewicz. Building a large annotated corpus of English: The Penn Treebank. *Computational Linguistics*, 19(2):313–330, 1993. URL https://aclanthology.org/J93-2004/.

Ryan McDonald, Joakim Nivre, Yvonne Quirmbach-Brundage, Yoav Goldberg, Dipanjan Das, Kuzman Ganchev, Keith Hall, Slav Petrov, Hao Zhang, Oscar Täckström, Claudia Bedini, Núria Bertomeu Castelló, and Jungmee Lee. Universal Dependency annotation for multilingual parsing. In Hinrich Schuetze, Pascale Fung, and Massimo Poesio (eds.), *Proceedings of the 51st Annual*

Meeting of the Association for Computational Linguistics (Volume 2: Short Papers), pp. 92–97, Sofia, Bulgaria, August 2013. Association for Computational Linguistics. URL https://aclanthology.org/P13-2017/.

Kevin Meng, David Bau, Alex J Andonian, and Yonatan Belinkov. Locating and editing factual associations in GPT. In Alice H. Oh, Alekh Agarwal, Danielle Belgrave, and Kyunghyun Cho (eds.), *Advances in Neural Information Processing Systems*, 2022. URL https://openreview.net/forum?id=-h6WAS6eE4.

Joakim Nivre, Marie-Catherine de Marneffe, Filip Ginter, Yoav Goldberg, Jan Hajič, Christopher D. Manning, Ryan McDonald, Slav Petrov, Sampo Pyysalo, Natalia Silveira, Reut Tsarfaty, and Daniel Zeman. Universal Dependencies v1: A multilingual treebank collection. In Nicoletta Calzolari, Khalid Choukri, Thierry Declerck, Sara Goggi, Marko Grobelnik, Bente Maegaard, Joseph Mariani, Helene Mazo, Asuncion Moreno, Jan Odijk, and Stelios Piperidis (eds.), *Proceedings of the Tenth International Conference on Language Resources and Evaluation (LREC'16)*, pp. 1659–1666, Portorož, Slovenia, May 2016. European Language Resources Association (ELRA). URL https://aclanthology.org/L16-1262/.

nostalgebraist. Interpreting GPT: The logit lens. https://www.lesswrong.com/posts/AcKRB8wDpdaN6v6ru/interpreting-gpt-the-logit-lens, 2020. LessWrong blog post.

Nina Panickssery, Nick Gabrieli, Julian Schulz, Meg Tong, Evan Hubinger, and Alexander Matt Turner. Steering llama 2 via contrastive activation addition, 2024. URL https://arxiv.org/abs/2312.06681.

Slav Petrov, Dipanjan Das, and Ryan McDonald. A universal part-of-speech tagset. In Nicoletta Calzolari, Khalid Choukri, Thierry Declerck, Mehmet Uğur Doğan, Bente Maegaard, Joseph Mariani, Asuncion Moreno, Jan Odijk, and Stelios Piperidis (eds.), *Proceedings of the Eighth International Conference on Language Resources and Evaluation (LREC'12)*, pp. 2089–2096, Istanbul, Turkey, May 2012. European Language Resources Association (ELRA). URL https://aclanthology.org/L12-1115/.

Sameer Pradhan, Alessandro Moschitti, Nianwen Xue, Olga Uryupina, and Yuchen Zhang. CoNLL-2012 shared task: Modeling multilingual unrestricted coreference in OntoNotes. In Sameer Pradhan, Alessandro Moschitti, and Nianwen Xue (eds.), *Joint Conference on EMNLP and CoNLL - Shared Task*, pp. 1–40, Jeju Island, Korea, July 2012. Association for Computational Linguistics. URL https://aclanthology.org/W12-4501/.

Alec Radford, Jeff Wu, Rewon Child, David Luan, Dario Amodei, and Ilya Sutskever. Language models are unsupervised multitask learners. *OpenAI blog*, 1(8):9, 2019.

Drew Reisinger, Rachel Rudinger, Francis Ferraro, Craig Harman, Kyle Rawlins, and Benjamin Van Durme. Semantic proto-roles. *Transactions of the Association for Computational Linguistics*, 3:475–488, 2015. doi: 10.1162/tacl_a_00152. URL https://aclanthology.org/Q15-1034/.

Anna Rogers, Olga Kovaleva, and Anna Rumshisky. A primer in BERTology: What we know about how BERT works. *Transactions of the Association for Computational Linguistics*, 8:842–866, 2020. doi: 10.1162/tacl_a_00349. URL https://aclanthology.org/2020.tacl-1.54/.

William Rudman, Catherine Chen, and Carsten Eickhoff. Outlier dimensions encode task specific knowledge. In Houda Bouamor, Juan Pino, and Kalika Bali (eds.), *Proceedings of the 2023 Conference on Empirical Methods in Natural Language Processing*, pp. 14596–14605, Singapore, December 2023. Association for Computational Linguistics. doi: 10.18653/v1/2023.emnlp-main.901. URL https://aclanthology.org/2023.emnlp-main.901/.

Oscar Skean, Md Rifat Arefin, Dan Zhao, Niket Nikul Patel, Jalal Naghiyev, Yann LeCun, and Ravid Shwartz-Ziv. Layer by layer: Uncovering hidden representations in language models. In *Forty-second International Conference on Machine Learning*, 2025. URL https://openreview.net/forum?id=WGXb7UdvTX.

Nishant Subramani, Nivedita Suresh, and Matthew Peters. Extracting latent steering vectors from pretrained language models. In Smaranda Muresan, Preslav Nakov, and Aline Villavicencio (eds.), *Findings of the Association for Computational Linguistics: ACL 2022*, pp. 566–581, Dublin, Ireland, May 2022. Association for Computational Linguistics. doi: 10.18653/v1/2022.findings-acl.48. URL https://aclanthology.org/2022.findings-acl.48/.

Nishant Subramani, Jason Eisner, Justin Svegliato, Benjamin Van Durme, Yu Su, and Sam Thomson. MICE for CATs: Model-internal confidence estimation for calibrating agents with tools. In Luis Chiruzzo, Alan Ritter, and Lu Wang (eds.), *Proceedings of the 2025 Conference of the Nations of the Americas Chapter of the Association for Computational Linguistics: Human Language Technologies (Volume 1: Long Papers)*, pp. 12362–12375, Albuquerque, New Mexico, April 2025. Association for Computational Linguistics. ISBN 979-8-89176-189-6. URL https://aclanthology.org/2025.naacl-long.615/.

Umut Sulubacak, Memduh Gokirmak, Francis Tyers, Çağrı Çöltekin, Joakim Nivre, and Gülşen Eryiğit. Universal Dependencies for Turkish. In Yuji Matsumoto and Rashmi Prasad (eds.), *Proceedings of COLING 2016, the 26th International Conference on Computational Linguistics: Technical Papers*, pp. 3444–3454, Osaka, Japan, December 2016. The COLING 2016 Organizing Committee. URL https://aclanthology.org/C16-1325/.

Mingjie Sun, Xinlei Chen, J Zico Kolter, and Zhuang Liu. Massive activations in large language models. In *First Conference on Language Modeling*, 2024. URL https://openreview.net/forum?id=F7aAhfitX6.

Ian Tenney, Dipanjan Das, and Ellie Pavlick. BERT rediscovers the classical NLP pipeline. In Anna Korhonen, David Traum, and Lluís Màrquez (eds.), *Proceedings of the 57th Annual Meeting of the Association for Computational Linguistics*, pp. 4593–4601, Florence, Italy, July 2019a. Association for Computational Linguistics. doi: 10.18653/v1/P19-1452. URL https://aclanthology.org/P19-1452/.

Ian Tenney, Patrick Xia, Berlin Chen, Alex Wang, Adam Poliak, R Thomas McCoy, Najoung Kim, Benjamin Van Durme, Sam Bowman, Dipanjan Das, and Ellie Pavlick. What do you learn from context? probing for sentence structure in contextualized word representations. In *International Conference on Learning Representations*, 2019b. URL https://openreview.net/forum?id=SJzSgnRcKX.

Erik F. Tjong Kim Sang and Fien De Meulder. Introduction to the CoNLL-2003 shared task: Language-independent named entity recognition. In *Proceedings of the Seventh Conference on Natural Language Learning at HLT-NAACL 2003*, pp. 142–147, 2003. URL https://aclanthology.org/W03-0419/.

Jesse Vig, Sebastian Gehrmann, Yonatan Belinkov, Sharon Qian, Daniel Nevo, Yaron Singer, and Stuart Shieber. Investigating gender bias in language models using causal mediation analysis. In H. Larochelle, M. Ranzato, R. Hadsell, M.F. Balcan, and H. Lin (eds.), *Advances in Neural Information Processing Systems*, volume 33, pp. 12388–12401. Curran Associates, Inc., 2020. URL https://proceedings.neurips.cc/paper_files/paper/2020/file/92650b2e92217715fe312e6fa7b90d82-Paper.pdf.

Elena Voita and Ivan Titov. Information-theoretic probing with minimum description length. In Bonnie Webber, Trevor Cohn, Yulan He, and Yang Liu (eds.), *Proceedings of the 2020 Conference on Empirical Methods in Natural Language Processing (EMNLP)*, pp. 183–196, Online, November 2020. Association for Computational Linguistics. doi: 10.18653/v1/2020.emnlp-main.14. URL https://aclanthology.org/2020.emnlp-main.14/.

Ivan Vulić, Edoardo Maria Ponti, Robert Litschko, Goran Glavaš, and Anna Korhonen. Probing pretrained language models for lexical semantics. In Bonnie Webber, Trevor Cohn, Yulan He, and Yang Liu (eds.), *Proceedings of the 2020 Conference on Empirical Methods in Natural Language Processing (EMNLP)*, pp. 7222–7240, Online, November 2020. Association for Computational Linguistics. doi: 10.18653/v1/2020.emnlp-main.586. URL https://aclanthology.org/2020.emnlp-main.586/.

BigScience Workshop. Bloom: A 176b-parameter open-access multilingual language model, 2023. URL https://arxiv.org/abs/2211.05100.

Linting Xue, Noah Constant, Adam Roberts, Mihir Kale, Rami Al-Rfou, Aditya Siddhant, Aditya Barua, and Colin Raffel. mT5: A massively multilingual pre-trained text-to-text transformer. In Kristina Toutanova, Anna Rumshisky, Luke Zettlemoyer, Dilek Hakkani-Tur, Iz Beltagy, Steven Bethard, Ryan Cotterell, Tanmoy Chakraborty, and Yichao Zhou (eds.), *Proceedings of the 2021 Conference of the North American Chapter of the Association for Computational Linguistics: Human Language Technologies*, pp. 483–498, Online, June 2021. Association for Computational Linguistics. doi: 10.18653/v1/2021.naacl-main.41. URL https://aclanthology.org/2021.naacl-main.41/.

Amir Zeldes. The GUM corpus: Creating multilayer resources in the classroom. *Language Resources and Evaluation*, 51(3):581–612, 2017. doi: http://dx.doi.org/10.1007/s10579-016-9343-x.

A Limitations

Representation Extraction for Decoder Models Our current approach for extracting word representations from decoder-only models uses the final subword token. This assumption is an intuitive and natural choice, but may not be optimal for all architectures and models. Future work could develop better extraction methods that account for subword tokenization effects and leverage attention patterns to create more accurate word-level representations.

Form and Function in Inflection Some languages contain cases where different grammatical functions share the same surface form (*e.g.*, , infinitive and non-past verb forms in English). We do not explicitly examine these cases in our classification experiments, but these ambiguities create opportunities to better examine how models separate form from function across languages.

Indirect Nature of Classifiers While our classifier methodology follows established best practices (Hewitt & Liang, 2019; Liu et al., 2019), we only detect correlations in hidden activations, not causal mechanisms.

Scope of Steering Experiments Our steering vector experiments measure changes in classifier performance rather than downstream model outputs. Evaluating effects on actual model generation would require more complex experimental designs to control for confounding factors and ensure that observed changes result from the intended representational modifications rather than other influences.

B Additional Related Work

B.1 Advanced Probing Methodologies

Beyond standard linear probes, there are many sophisticated approaches to understand model representations. Amnesic probing (Elazar et al., 2021) removes specific information from representations to test whether it's necessary for downstream tasks. Minimum description length probes (Voita & Titov, 2020) balance probe complexity with performance to avoid overfitting. Causal abstraction (Geiger et al., 2021) aims to establish causal rather than merely correlational relationships between representations and linguistic properties. Recently, Subramani et al. (2025) find that decoding from activations directly using the Logit Lens can be used to learn confidence estimators for tool-calling agents (nostalgebraist, 2020).

B.2 Model Manipulation and Steering

Steering vectors demonstrate that specific directions in activation space correspond to high-level behavioral changes (Subramani et al., 2022). Building on this, Panickssery et al. (2024) achieves behavioral control by adding activation differences between contrasting examples. Li et al. (2023) introduce inference-time intervention, a method that shifts model activations during inference across limited attention heads to control model behavior. While these methods operate in activation space, task vectors enable arithmetic operations on model capabilities by manipulating weight space (Ilharco et al., 2023).

Recent work has also examined how multilingual models like mT5 and ByT5 encode morphological information differently across languages (Dang et al., 2024), finding that tokenization strategies significantly impact morphological representation quality, particularly for morphologically rich languages.

C Probe Details

In this appendix we provide implementation details for the linear regression and two-layer multi-layer perceptron (MLP) probes used throughout our experiments. These classifiers are trained on frozen residual-stream activations from each layer to predict the labels of our linguistic tasks, lemma identity and inflectional features.

Training details. We stratify each dataset into train, validation, and test splits. Probes are trained on the training split, hyperparameters are selected using the validation split, and we report accuracy and macro F1 on the held-out test split. For the linear regression probe we apply ridge regularization with $\lambda = 0.01$ and solve equation (5) in closed form. For the MLP probe we use a hidden dimension of 64, a learning rate of 0.001, weight decay of 0.01, and train for up to 100 epochs with early stopping based on validation loss, optimizing cross-entropy with AdamW. Both probes share the same data splits to enable fair comparison.

C.1 Linear Regression Classifier

Consistent with best practices for probing (Hewitt & Liang, 2019; Liu et al., 2019), we use a ridge-regularized linear regression classifier. Given training representations $X_{\text{train}} \in \mathbb{R}^{m \times d}$ and one-hot encoded labels $Y_{\text{train}} \in \mathbb{R}^{m \times c}$, the optimal weight matrix $W \in \mathbb{R}^{d \times c}$ is obtained in closed form as

$$W = \left(X_{\text{train}}^{\top} X_{\text{train}} + \lambda I\right)^{-1} X_{\text{train}}^{\top} Y_{\text{train}}, \tag{5}$$

where λ controls the strength of ℓ_2 regularization and I is the identity matrix. Predictions on test representations X_{test} are then given by $\hat{Y}_{\text{test}} = X_{\text{test}} W$.

C.2 MLP Classifier

To test for non-linear separability, we train a simple two-layer MLP with ReLU activation. The classifier computes

$$\hat{Y} = \text{softmax}\Big(\text{ReLU}(XW_1)W_2\Big), \tag{6}$$

where $W_1 \in \mathbb{R}^{d \times h}$ and $W_2 \in \mathbb{R}^{h \times c}$ are learned weight matrices, h is the hidden dimension (we use $h = 64$), and biases are omitted for brevity. Two-layer MLPs with ReLU activation are universal function approximators capable of representing any continuous function to arbitrary precision given sufficient width (Hornik et al., 1989). We train the MLP with cross-entropy loss using the same splits and optimization hyperparameters described above.

D Linguistic Task Definitions

We probe eight linguistic tasks originally introduced by Tenney et al. (2019a) that span the classical NLP pipeline. Here we provide formal definitions for each task:

Part-of-Speech tagging (POS). This task assigns each word a grammatical category such as noun, verb, adjective, or adverb, following the Universal Dependencies tagset (Petrov et al., 2012). POS tagging is fundamental to syntactic analysis and serves as input to many downstream NLP tasks.

Constituency parsing. This task identifies the hierarchical phrase structure of sentences by grouping words into nested constituents such as noun phrases, verb phrases, and sentences (Marcus et al., 1993). The output is typically represented as a parse tree showing how smaller units combine to form larger syntactic structures.

Dependency parsing. This task predicts syntactic head-dependent relations between words, such as subject-verb and modifier-head relationships, following Universal Dependencies guidelines (Nivre et al., 2016). Each word is linked to exactly one head (except the root), forming a directed tree structure that captures grammatical relations.

Named Entity Recognition (NER). This task identifies and classifies named entities such as persons, organizations, locations, and dates into predefined categories (Tjong Kim Sang & De Meulder, 2003). NER bridges syntactic and semantic analysis by identifying referential expressions that denote real-world entities.

Semantic Role Labeling (SRL). This task assigns semantic roles such as agent, patient, instrument, or location to arguments of predicates in a sentence (Gildea & Jurafsky, 2002). SRL captures the underlying semantic relationships between predicates and their arguments, abstracting away from surface syntactic variations.

Semantic Proto-Roles (SPR). This task predicts fine-grained semantic properties of predicate arguments, such as whether an argument is sentient, undergoes a change of state, or is volitional (Reisinger et al., 2015). SPR provides a more nuanced characterization of semantic roles through scalar properties rather than categorical labels.

Coreference resolution. This task determines which expressions in a text refer to the same real-world entity, linking pronouns and noun phrases to their antecedents (Pradhan et al., 2012). Coreference resolution is essential for understanding discourse coherence and tracking entities across sentences.

Relation extraction. This task identifies semantic relationships between entity mentions, such as organization-location or person-affiliation relations, typically across sentence boundaries (Hendrickx et al., 2010). Relation extraction connects named entities through typed semantic links, enabling structured knowledge representation.

These tasks form the classical NLP pipeline described by (Tenney et al., 2019a), progressing from syntactic analysis (POS, constituency, dependencies) through semantic interpretation (NER, SRL, SPR) to discourse-level understanding (coreference, relations).

E Full Results for the Classical NLP Pipeline

The full heatmaps and summary statistics for pipeline analyses across all models are shown in Figures 7–11. These figures show model-by-layer accuracy/selectivity patterns and the expected layer/center-of-gravity summaries reported in the main text.

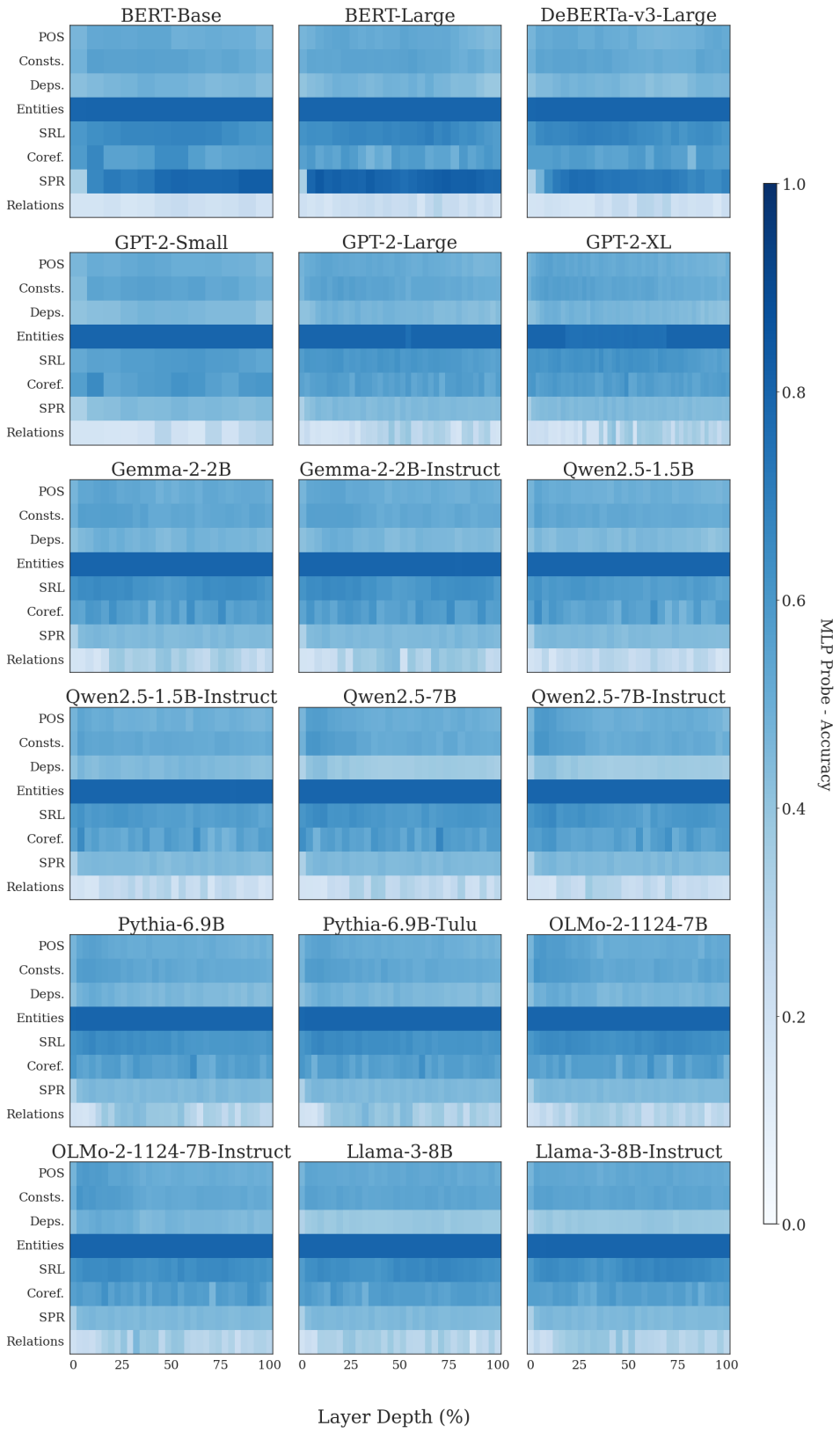

Figure 7: Full heatmaps for MLP probe accuracy across all tasks, models, and layers. Rows show tasks; columns show models; each plot shows accuracy by layer depth.

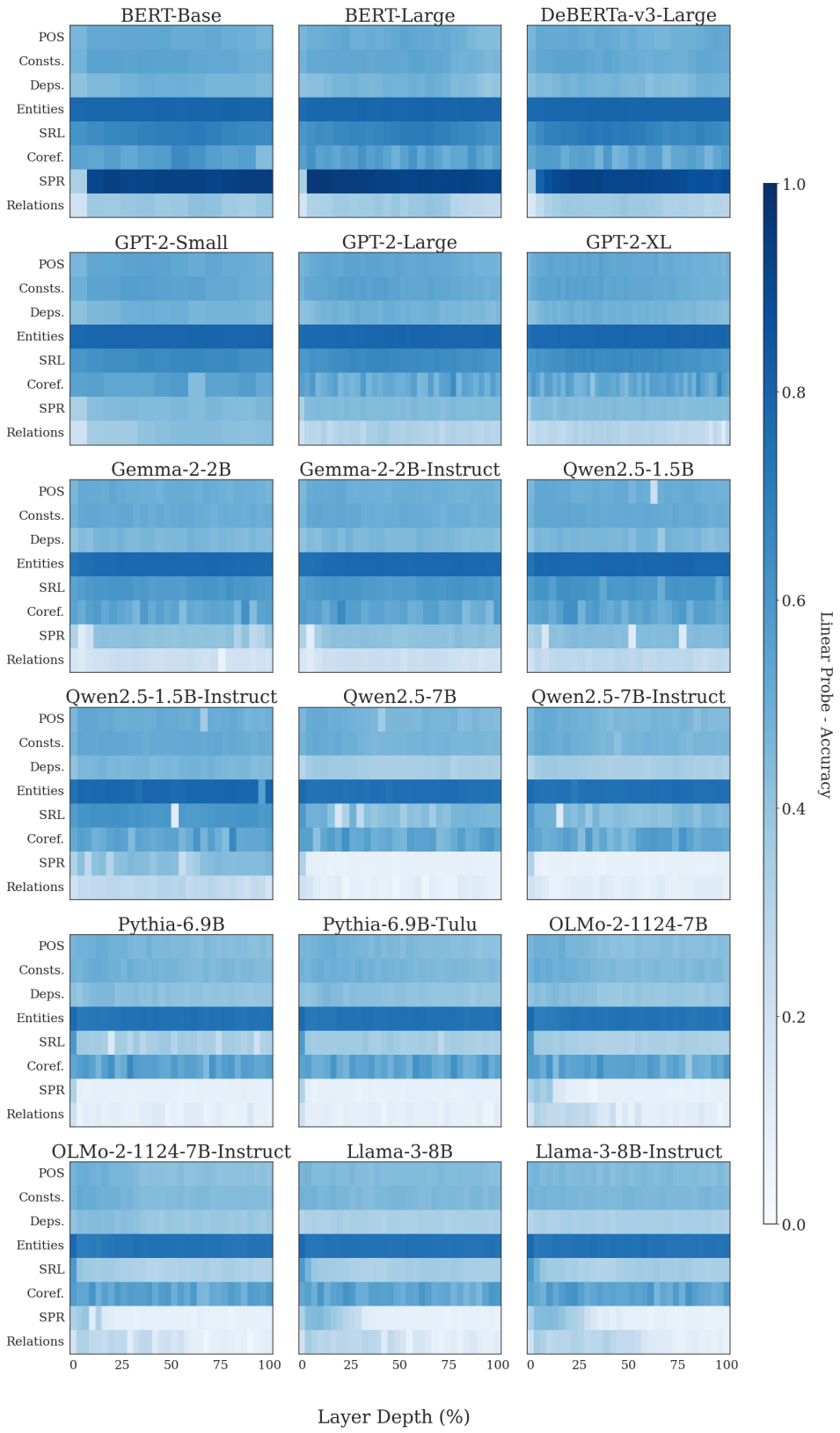

Figure 8: Full heatmaps for linear probe accuracy across all tasks, models, and layers. Trends mirror the MLP version but with stronger model-size effects in deeper layers.

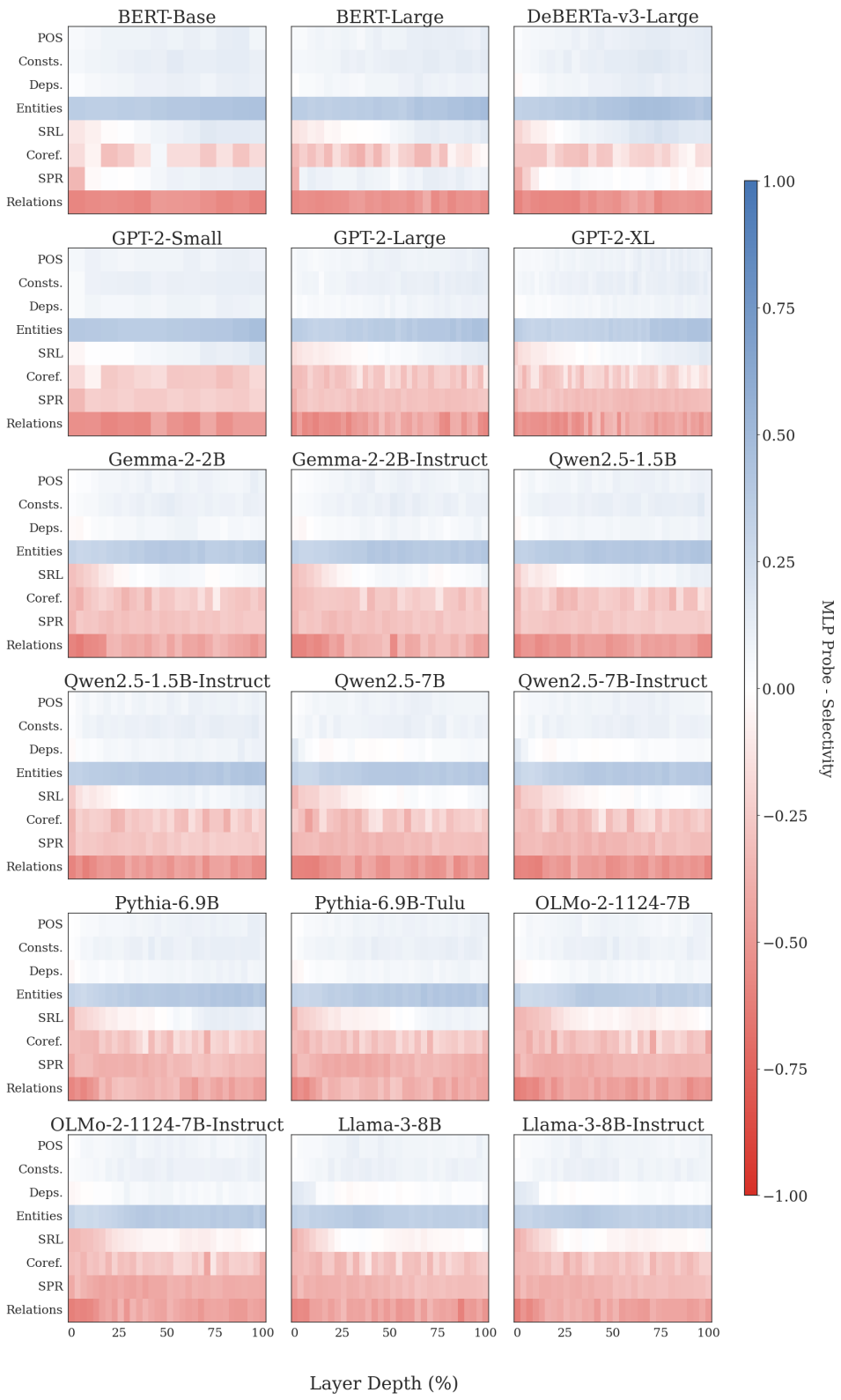

Figure 9: Full heatmaps for MLP probe selectivity (real vs. control task accuracy).

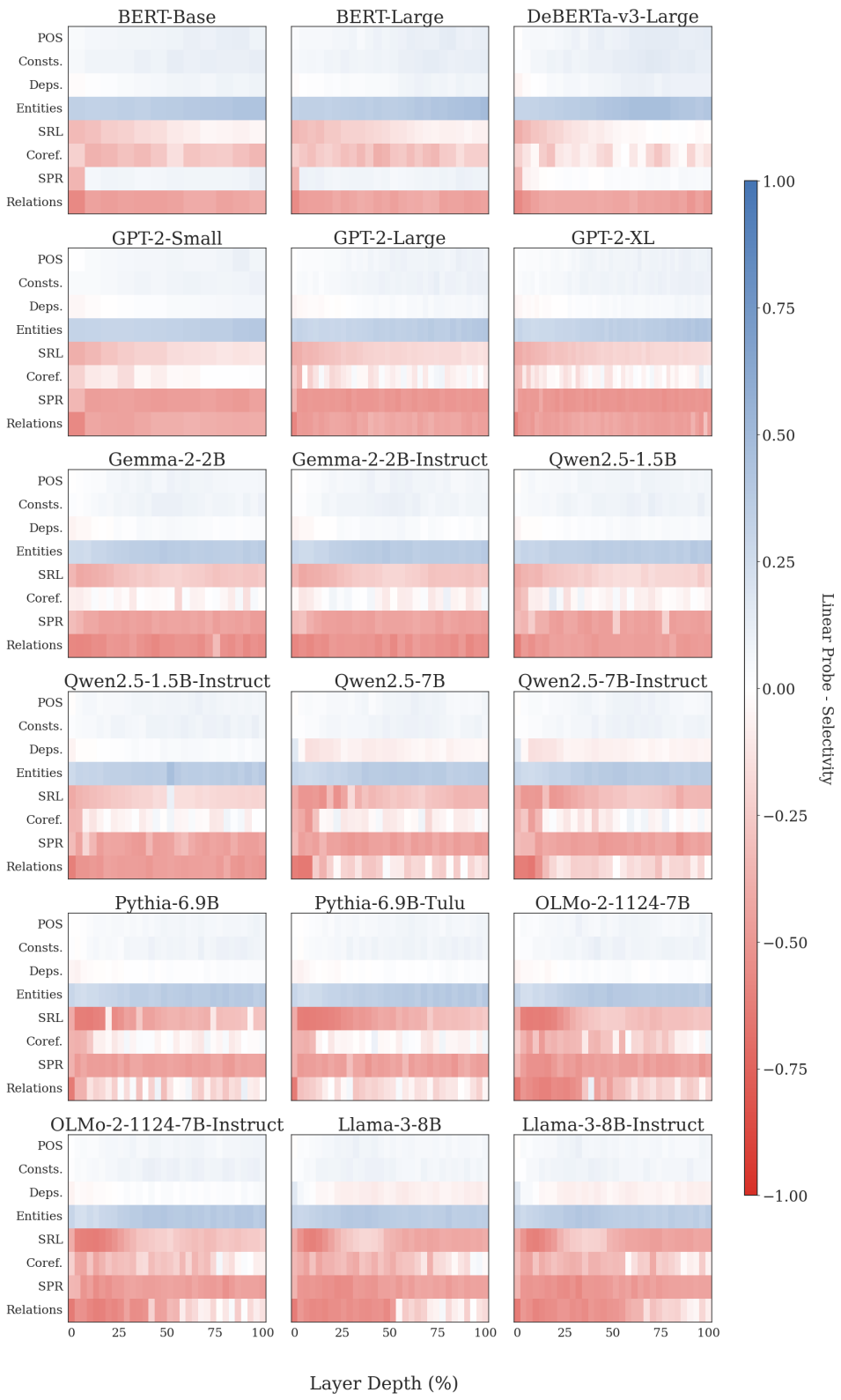

Figure 10: Full heatmaps for linear probe selectivity (real vs. control task accuracy).

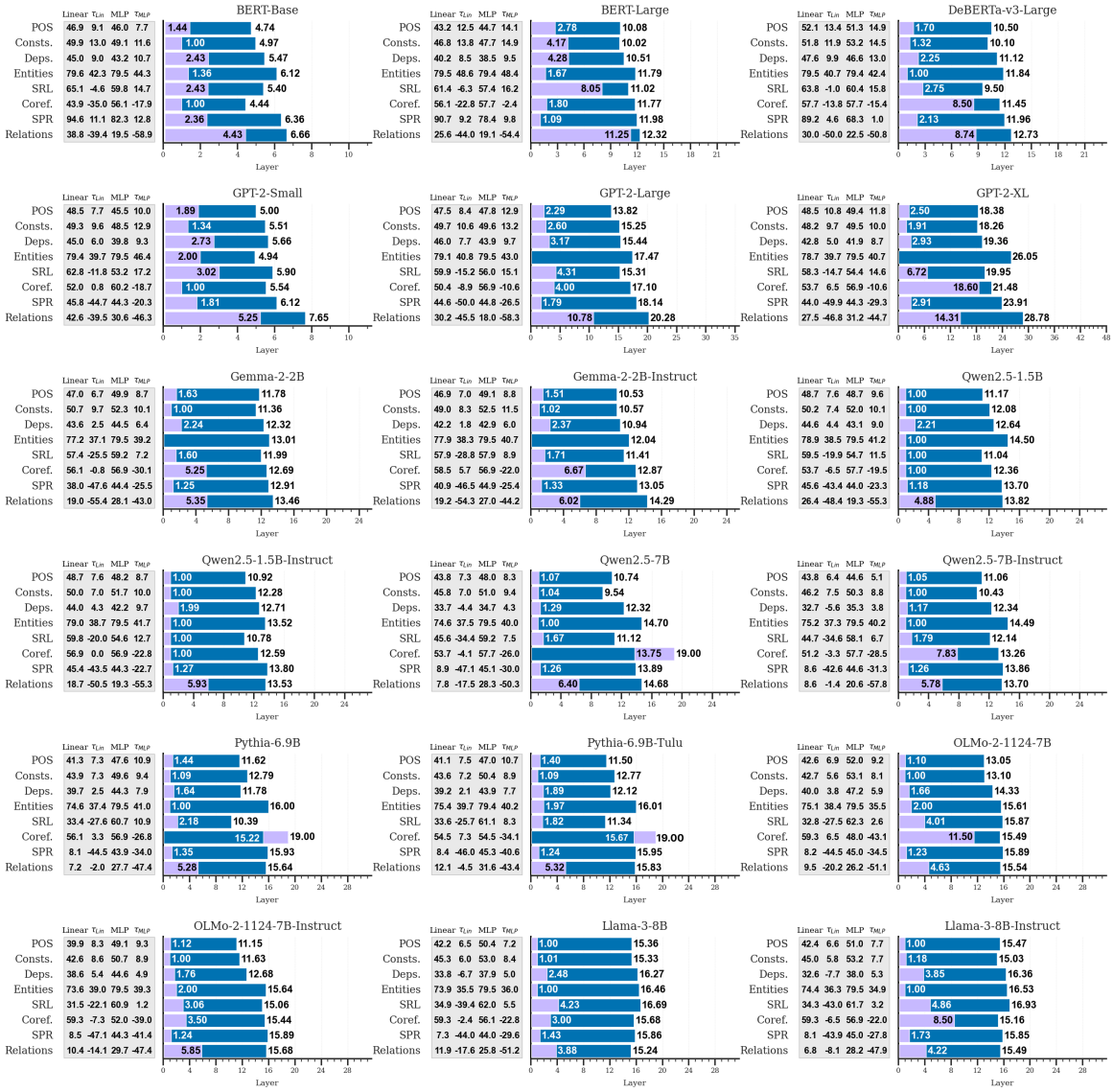

Figure 11: Expected Layer and Center of Gravity plots with τ_{lin} and τ_{MLP} selectivity scores for all models.

F Full Lemma and Inflection Probe Results

We provide the full, non-averaged results for the linguistic probing tasks (lemma identity and inflectional features) for every individual model. Figure 12 shows the detailed breakdown for English models, and Figure 13 presents the results for all six languages.

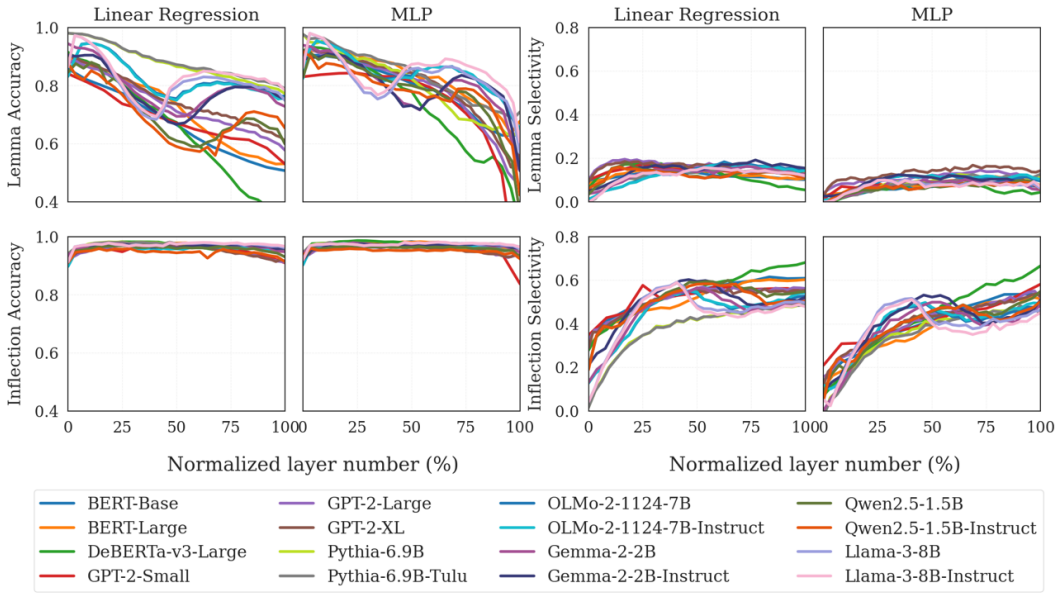

Figure 12: Full lemma and inflection probing results for English, showing individual curves for every model. Columns show prediction accuracy (Linear vs. MLP probes) and selectivity scores (linguistic minus control accuracy).

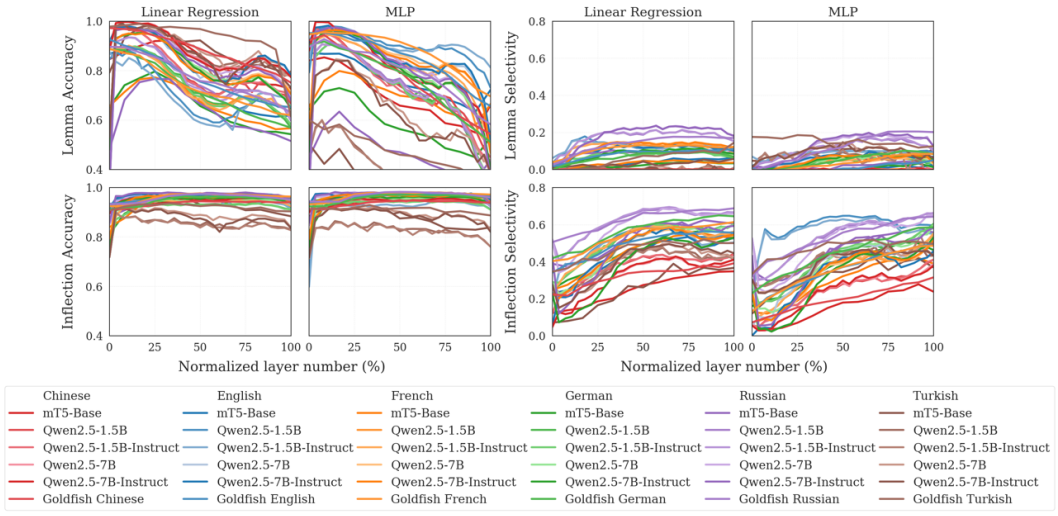

Figure 13: Full cross-linguistic probing results showing individual curves for every model within each language. Columns show lemma and inflection accuracy (Linear vs. MLP) followed by selectivity scores.

G Detailed Layer-wise Tables for Lemma and Inflection Results

This section contains detailed tables for layer-wise accuracy and selectivity across all models and languages.

Table 2: English Accuracy (Linear Probes) Across Layer Depths

Model	Task	0%	25%	50%	75%	100%
BERT-Base	Inflection	0.934	0.971	0.977	0.966	0.951
	Lexeme	0.858	0.773	0.665	0.564	0.507
BERT-Large	Inflection	0.938	0.972	0.978	0.966	0.949
	Lexeme	0.896	0.820	0.737	0.585	0.531
DeBERTa-v3-Large	Inflection	0.939	0.982	0.972	0.960	0.955
	Lexeme	0.914	0.805	0.673	0.482	0.309
GPT-2-Large	Inflection	0.927	0.970	0.971	0.946	0.912
	Lexeme	0.874	0.818	0.711	0.665	0.577
GPT-2-Small	Inflection	0.939	0.948	0.971	0.956	0.909
	Lexeme	0.840	0.737	0.671	0.618	0.530
GPT-2-XL	Inflection	0.929	0.974	0.973	0.946	0.915
	Lexeme	0.906	0.827	0.737	0.690	0.609
Gemma-2-2B	Inflection	0.936	0.974	0.963	0.972	0.948
	Lexeme	0.944	0.817	0.694	0.792	0.728
Gemma-2-2B-Instruct	Inflection	0.917	0.971	0.960	0.972	0.960
	Lexeme	0.904	0.802	0.667	0.791	0.752
Llama-3-8B	Inflection	0.912	0.971	0.974	0.976	0.962
	Lexeme	0.864	0.794	0.796	0.816	0.749
Llama-3-8B-Instruct	Inflection	0.913	0.972	0.974	0.977	0.967
	Lexeme	0.864	0.803	0.812	0.839	0.783
OLMo-2-1124-7B	Inflection	0.897	0.970	0.959	0.961	0.965
	Lexeme	0.832	0.883	0.755	0.808	0.763
OLMo-2-1124-7B-Instruct	Inflection	0.897	0.970	0.958	0.962	0.961
	Lexeme	0.832	0.881	0.749	0.806	0.757
Pythia-6.9B	Inflection	0.942	0.982	0.974	0.966	0.953
	Lexeme	0.980	0.928	0.865	0.829	0.772
Pythia-6.9B-Tulu	Inflection	0.941	0.980	0.975	0.968	0.954
	Lexeme	0.980	0.928	0.872	0.841	0.789
Qwen2.5-1.5B	Inflection	0.913	0.969	0.959	0.961	0.930
	Lexeme	0.845	0.799	0.610	0.654	0.599
Qwen2.5-1.5B-Instruct	Inflection	0.910	0.957	0.944	0.949	0.914
	Lexeme	0.876	0.768	0.590	0.647	0.654

Table 3: English Selectivity (Linear Probes) Across Layer Depths

Model	Task	0%	25%	50%	75%	100%
BERT-Base	Inflection	0.348	0.486	0.556	0.596	0.609
	Lexeme	0.094	0.132	0.134	0.114	0.101
BERT-Large	Inflection	0.292	0.459	0.520	0.598	0.603
	Lexeme	0.083	0.145	0.148	0.119	0.107
DeBERTa-v3-Large	Inflection	0.279	0.471	0.545	0.644	0.681
	Lexeme	0.062	0.183	0.158	0.097	0.054
GPT-2-Large	Inflection	0.324	0.489	0.563	0.550	0.562
	Lexeme	0.099	0.183	0.162	0.161	0.121
GPT-2-Small	Inflection	0.347	0.576	0.541	0.558	0.547
	Lexeme	0.100	0.171	0.152	0.134	0.121
GPT-2-XL	Inflection	0.289	0.488	0.549	0.547	0.553
	Lexeme	0.092	0.172	0.172	0.162	0.135
Gemma-2-2B	Inflection	0.131	0.466	0.565	0.464	0.512
	Lexeme	0.036	0.132	0.136	0.161	0.128
Gemma-2-2B-Instruct	Inflection	0.210	0.517	0.594	0.487	0.522
	Lexeme	0.052	0.157	0.144	0.184	0.154
Llama-3-8B	Inflection	0.041	0.516	0.482	0.474	0.497
	Lexeme	-0.003	0.132	0.146	0.140	0.117
Llama-3-8B-Instruct	Inflection	0.042	0.508	0.473	0.453	0.478
	Lexeme	-0.003	0.131	0.146	0.144	0.119
OLMo-2-1124-7B	Inflection	0.128	0.440	0.538	0.476	0.528
	Lexeme	0.011	0.104	0.152	0.170	0.144
OLMo-2-1124-7B-Instruct	Inflection	0.127	0.443	0.545	0.483	0.543
	Lexeme	0.011	0.104	0.149	0.164	0.144
Pythia-6.9B	Inflection	0.017	0.347	0.416	0.457	0.484
	Lexeme	-0.002	0.117	0.134	0.140	0.141
Pythia-6.9B-Tulu	Inflection	0.016	0.348	0.419	0.454	0.492
	Lexeme	-0.002	0.118	0.137	0.143	0.150
Qwen2.5-1.5B	Inflection	0.199	0.483	0.589	0.566	0.548
	Lexeme	0.034	0.146	0.117	0.129	0.108
Qwen2.5-1.5B-Instruct	Inflection	0.189	0.474	0.581	0.541	0.503
	Lexeme	0.061	0.143	0.113	0.129	0.112

Table 4: English Accuracy (MLP Probes) Across Layer Depths

Model	Task	0%	25%	50%	75%	100%
BERT-Base	Inflection	0.941	0.978	0.983	0.975	0.960
	Lexeme	0.906	0.888	0.808	0.719	0.629
BERT-Large	Inflection	0.943	0.977	0.981	0.973	0.958
	Lexeme	0.920	0.904	0.843	0.762	0.677
DeBERTa-v3-Large	Inflection	0.944	0.986	0.976	0.971	0.957
	Lexeme	0.920	0.885	0.781	0.574	0.318
GPT-2-Large	Inflection	0.930	0.964	0.964	0.952	0.937
	Lexeme	0.892	0.878	0.825	0.719	0.552
GPT-2-Small	Inflection	0.943	0.963	0.965	0.957	0.837
	Lexeme	0.830	0.843	0.817	0.705	0.075
GPT-2-XL	Inflection	0.929	0.965	0.963	0.948	0.937
	Lexeme	0.906	0.884	0.844	0.734	0.571
Gemma-2-2B	Inflection	0.940	0.977	0.970	0.975	0.946
	Lexeme	0.939	0.868	0.732	0.812	0.506
Gemma-2-2B-Instruct	Inflection	0.919	0.973	0.965	0.973	0.960
	Lexeme	0.890	0.874	0.731	0.831	0.508
Llama-3-8B	Inflection	0.920	0.972	0.977	0.976	0.958
	Lexeme	0.863	0.808	0.857	0.840	0.568
Llama-3-8B-Instruct	Inflection	0.920	0.972	0.977	0.977	0.964
	Lexeme	0.863	0.821	0.873	0.870	0.605
OLMo-2-1124-7B	Inflection	0.903	0.974	0.970	0.975	0.964
	Lexeme	0.825	0.877	0.833	0.845	0.621
OLMo-2-1124-7B-Instruct	Inflection	0.903	0.975	0.968	0.973	0.964
	Lexeme	0.825	0.880	0.825	0.847	0.650
Pythia-6.9B	Inflection	0.940	0.973	0.971	0.959	0.959
	Lexeme	0.976	0.891	0.823	0.683	0.655
Pythia-6.9B-Tulu	Inflection	0.944	0.973	0.970	0.963	0.961
	Lexeme	0.976	0.904	0.858	0.752	0.709
Qwen2.5-1.5B	Inflection	0.919	0.967	0.963	0.962	0.929
	Lexeme	0.829	0.864	0.800	0.777	0.356
Qwen2.5-1.5B-Instruct	Inflection	0.935	0.957	0.952	0.952	0.923
	Lexeme	0.916	0.841	0.779	0.789	0.423

Table 5: English Selectivity (MLP Probes) Across Layer Depths

Model	Task	0%	25%	50%	75%	100%
BERT-Base	Inflection	0.139	0.307	0.416	0.505	0.536
	Lexeme	0.025	0.057	0.069	0.084	0.068
BERT-Large	Inflection	0.104	0.294	0.386	0.496	0.514
	Lexeme	0.028	0.084	0.088	0.106	0.074
DeBERTa-v3-Large	Inflection	0.071	0.313	0.428	0.582	0.666
	Lexeme	0.005	0.061	0.096	0.065	0.043
GPT-2-Large	Inflection	0.157	0.323	0.446	0.487	0.521
	Lexeme	0.040	0.093	0.123	0.138	0.115
GPT-2-Small	Inflection	0.210	0.342	0.410	0.470	0.581
	Lexeme	0.012	0.077	0.094	0.107	0.061
GPT-2-XL	Inflection	0.118	0.334	0.433	0.491	0.527
	Lexeme	0.027	0.110	0.145	0.163	0.142
Gemma-2-2B	Inflection	0.002	0.360	0.499	0.395	0.483
	Lexeme	-0.007	0.067	0.090	0.088	0.054
Gemma-2-2B-Instruct	Inflection	0.089	0.393	0.523	0.404	0.509
	Lexeme	0.026	0.102	0.111	0.100	0.058
Llama-3-8B	Inflection	0.050	0.454	0.414	0.402	0.463
	Lexeme	-0.001	0.098	0.079	0.084	0.060
Llama-3-8B-Instruct	Inflection	0.050	0.442	0.400	0.364	0.451
	Lexeme	-0.002	0.098	0.074	0.084	0.069
OLMo-2-1124-7B	Inflection	0.118	0.363	0.470	0.426	0.483
	Lexeme	0.007	0.088	0.121	0.109	0.095
OLMo-2-1124-7B-Instruct	Inflection	0.118	0.371	0.476	0.434	0.493
	Lexeme	0.007	0.094	0.122	0.119	0.103
Pythia-6.9B	Inflection	-0.025	0.301	0.404	0.444	0.451
	Lexeme	-0.005	0.064	0.096	0.110	0.113
Pythia-6.9B-Tulu	Inflection	-0.021	0.294	0.394	0.438	0.445
	Lexeme	-0.005	0.057	0.092	0.112	0.126
Qwen2.5-1.5B	Inflection	0.085	0.325	0.456	0.455	0.549
	Lexeme	-0.007	0.053	0.072	0.082	0.062
Qwen2.5-1.5B-Instruct	Inflection	0.046	0.337	0.460	0.440	0.502
	Lexeme	-0.012	0.064	0.082	0.082	0.058

Table 6: Probing Results for Chinese

(a) Accuracy (Linear Probes)

Model	Task	0%	25%	50%	75%	100%
Goldfish Chinese (Chinese)	Inflection	0.911	0.928	0.944	0.942	0.941
	Lexeme	0.972	0.941	0.887	0.824	0.751
Qwen2.5-1.5B (Chinese)	Inflection	0.898	0.948	0.949	0.950	0.946
	Lexeme	0.883	0.905	0.735	0.743	0.667
Qwen2.5-1.5B-Instruct (Chinese)	Inflection	0.897	0.948	0.949	0.950	0.948
	Lexeme	0.883	0.907	0.729	0.748	0.678
Qwen2.5-7B (Chinese)	Inflection	0.893	0.957	0.951	0.956	0.950
	Lexeme	0.883	0.983	0.844	0.828	0.776
Qwen2.5-7B-Instruct (Chinese)	Inflection	0.893	0.957	0.950	0.956	0.949
	Lexeme	0.883	0.981	0.839	0.823	0.773
mT5-Base (Chinese)	Inflection	0.901	0.933	0.945	0.941	0.943
	Lexeme	0.846	0.919	0.863	0.757	0.727

(b) Selectivity (Linear Probes)

Model	Task	0%	25%	50%	75%	100%
Goldfish Chinese (Chinese)	Inflection	0.223	0.292	0.346	0.356	0.391
	Lexeme	-0.000	-0.001	-0.002	-0.001	-0.003
Qwen2.5-1.5B (Chinese)	Inflection	0.122	0.345	0.429	0.412	0.441
	Lexeme	-0.000	-0.000	-0.002	-0.002	-0.003
Qwen2.5-1.5B-Instruct (Chinese)	Inflection	0.122	0.345	0.430	0.412	0.437
	Lexeme	-0.000	-0.001	-0.003	-0.001	-0.002
Qwen2.5-7B (Chinese)	Inflection	0.047	0.250	0.387	0.386	0.408
	Lexeme	-0.000	0.000	-0.001	0.000	-0.000
Qwen2.5-7B-Instruct (Chinese)	Inflection	0.048	0.250	0.392	0.387	0.411
	Lexeme	-0.000	-0.000	-0.001	0.000	-0.001
mT5-Base (Chinese)	Inflection	0.123	0.186	0.274	0.321	0.348
	Lexeme	0.001	0.000	-0.001	0.000	-0.003

(c) Accuracy (MLP Probes)

Model	Task	0%	25%	50%	75%	100%
Goldfish Chinese (Chinese)	Inflection	0.913	0.930	0.946	0.944	0.939
	Lexeme	0.922	0.874	0.797	0.652	0.543
Qwen2.5-1.5B (Chinese)	Inflection	0.896	0.947	0.943	0.950	0.942
	Lexeme	0.882	0.869	0.738	0.695	0.449
Qwen2.5-1.5B-Instruct (Chinese)	Inflection	0.896	0.941	0.942	0.950	0.943
	Lexeme	0.883	0.864	0.719	0.691	0.383
Qwen2.5-7B (Chinese)	Inflection	0.899	0.952	0.947	0.955	0.946
	Lexeme	0.881	0.951	0.795	0.749	0.471
Qwen2.5-7B-Instruct (Chinese)	Inflection	0.900	0.952	0.948	0.955	0.943
	Lexeme	0.881	0.950	0.791	0.750	0.475
mT5-Base (Chinese)	Inflection	0.907	0.938	0.947	0.942	0.948
	Lexeme	0.841	0.796	0.658	0.587	0.661

(d) Selectivity (MLP Probes)

Model	Task	0%	25%	50%	75%	100%
Goldfish Chinese (Chinese)	Inflection	0.072	0.153	0.198	0.252	0.315
	Lexeme	-0.001	-0.039	-0.049	-0.064	-0.047
Qwen2.5-1.5B (Chinese)	Inflection	0.058	0.168	0.280	0.305	0.411
	Lexeme	0.000	-0.001	-0.006	-0.001	0.002
Qwen2.5-1.5B-Instruct (Chinese)	Inflection	0.059	0.164	0.290	0.301	0.411
	Lexeme	0.000	0.002	-0.012	-0.000	-0.002
Qwen2.5-7B (Chinese)	Inflection	0.061	0.136	0.287	0.312	0.388
	Lexeme	-0.001	-0.001	-0.007	-0.008	0.000
Qwen2.5-7B-Instruct (Chinese)	Inflection	0.055	0.135	0.298	0.314	0.379
	Lexeme	-0.001	-0.003	-0.006	-0.004	-0.000
mT5-Base (Chinese)	Inflection	0.055	0.070	0.179	0.238	0.238
	Lexeme	0.003	-0.008	-0.013	-0.006	-0.011

Table 7: Probing Results for English

(a) Accuracy (Linear Probes)

Model	Task	0%	25%	50%	75%	100%
Goldfish English (English)	Inflection	0.934	0.956	0.972	0.964	0.949
	Lexeme	0.926	0.859	0.755	0.690	0.652
Qwen2.5-1.5B (English)	Inflection	0.913	0.969	0.959	0.961	0.930
	Lexeme	0.845	0.799	0.610	0.654	0.599
Qwen2.5-1.5B-Instruct (English)	Inflection	0.910	0.957	0.944	0.949	0.914
	Lexeme	0.876	0.768	0.590	0.647	0.654
Qwen2.5-7B (English)	Inflection	0.915	0.977	0.966	0.973	0.958
	Lexeme	0.916	0.952	0.769	0.808	0.781
Qwen2.5-7B-Instruct (English)	Inflection	0.915	0.977	0.964	0.973	0.957
	Lexeme	0.916	0.950	0.791	0.810	0.781
mT5-Base (English)	Inflection	0.920	0.966	0.969	0.966	0.958
	Lexeme	0.868	0.862	0.731	0.634	0.619

(b) Selectivity (Linear Probes)

Model	Task	0%	25%	50%	75%	100%
Goldfish English (English)	Inflection	0.341	0.437	0.522	0.549	0.556
	Lexeme	0.017	0.073	0.096	0.100	0.110
Qwen2.5-1.5B (English)	Inflection	0.199	0.483	0.589	0.566	0.548
	Lexeme	0.034	0.146	0.117	0.129	0.108
Qwen2.5-1.5B-Instruct (English)	Inflection	0.189	0.474	0.581	0.541	0.503
	Lexeme	0.061	0.143	0.113	0.129	0.112
Qwen2.5-7B (English)	Inflection	0.059	0.383	0.538	0.533	0.523
	Lexeme	-0.006	0.098	0.121	0.131	0.099
Qwen2.5-7B-Instruct (English)	Inflection	0.059	0.392	0.542	0.531	0.528
	Lexeme	-0.006	0.098	0.116	0.129	0.100
mT5-Base (English)	Inflection	0.229	0.348	0.462	0.533	0.530
	Lexeme	0.003	0.005	0.047	0.053	0.063

(c) Accuracy (MLP Probes)

Model	Task	0%	25%	50%	75%	100%
Goldfish English (English)	Inflection	0.937	0.962	0.976	0.971	0.964
	Lexeme	0.952	0.922	0.871	0.790	0.656
Qwen2.5-1.5B (English)	Inflection	0.666	0.956	0.956	0.961	0.929
	Lexeme	0.792	0.959	0.901	0.886	0.731
Qwen2.5-1.5B-Instruct (English)	Inflection	0.598	0.922	0.928	0.942	0.913
	Lexeme	0.852	0.939	0.880	0.900	0.812
Qwen2.5-7B (English)	Inflection	0.919	0.970	0.963	0.970	0.953
	Lexeme	0.913	0.935	0.831	0.818	0.506
Qwen2.5-7B-Instruct (English)	Inflection	0.930	0.976	0.970	0.976	0.951
	Lexeme	0.913	0.933	0.824	0.818	0.521
mT5-Base (English)	Inflection	NaN	NaN	NaN	NaN	NaN
	Lexeme	0.871	0.845	0.744	0.686	0.722

(d) Selectivity (MLP Probes)

Model	Task	0%	25%	50%	75%	100%
Goldfish English (English)	Inflection	0.131	0.272	0.371	0.438	0.493
	Lexeme	0.006	-0.021	0.005	0.031	0.050
Qwen2.5-1.5B (English)	Inflection	0.248	0.588	0.647	0.625	0.595
	Lexeme	0.019	0.085	0.096	0.101	0.090
Qwen2.5-1.5B-Instruct (English)	Inflection	0.187	0.571	0.629	0.608	0.549
	Lexeme	0.069	0.090	0.097	0.100	0.087
Qwen2.5-7B (English)	Inflection	0.051	0.282	0.456	0.457	0.507
	Lexeme	-0.008	0.039	0.070	0.073	0.061
Qwen2.5-7B-Instruct (English)	Inflection	0.001	0.229	0.424	0.416	0.457
	Lexeme	-0.008	0.042	0.072	0.067	0.068
mT5-Base (English)	Inflection	NaN	NaN	NaN	NaN	NaN
	Lexeme	-0.012	-0.023	0.003	0.011	0.026

Table 8: Probing Results for French

(a) Accuracy (Linear Probes)

Model	Task	0%	25%	50%	75%	100%
Goldfish French (French)	Inflection	0.924	0.959	0.976	0.970	0.963
	Lexeme	0.888	0.813	0.714	0.665	0.619
Qwen2.5-1.5B (French)	Inflection	0.792	0.947	0.954	0.952	0.928
	Lexeme	0.541	0.850	0.696	0.696	0.602
Qwen2.5-1.5B-Instruct (French)	Inflection	0.792	0.945	0.951	0.949	0.925
	Lexeme	0.541	0.845	0.687	0.690	0.611
Qwen2.5-7B (French)	Inflection	0.793	0.966	0.965	0.964	0.945
	Lexeme	0.541	0.943	0.801	0.769	0.714
Qwen2.5-7B-Instruct (French)	Inflection	0.793	0.963	0.962	0.961	0.941
	Lexeme	0.541	0.942	0.790	0.760	0.706
mT5-Base (French)	Inflection	0.840	0.943	0.967	0.961	0.944
	Lexeme	0.656	0.773	0.674	0.596	0.567

(b) Selectivity (Linear Probes)

Model	Task	0%	25%	50%	75%	100%
Goldfish French (French)	Inflection	0.403	0.497	0.581	0.585	0.613
	Lexeme	0.039	0.109	0.132	0.131	0.122
Qwen2.5-1.5B (French)	Inflection	0.244	0.463	0.576	0.559	0.561
	Lexeme	0.002	0.137	0.126	0.132	0.088
Qwen2.5-1.5B-Instruct (French)	Inflection	0.244	0.467	0.582	0.565	0.562
	Lexeme	0.002	0.137	0.126	0.132	0.092
Qwen2.5-7B (French)	Inflection	0.228	0.370	0.538	0.545	0.540
	Lexeme	0.003	0.116	0.145	0.139	0.112
Qwen2.5-7B-Instruct (French)	Inflection	0.228	0.375	0.545	0.552	0.544
	Lexeme	0.002	0.118	0.143	0.138	0.112
mT5-Base (French)	Inflection	0.248	0.386	0.495	0.548	0.530
	Lexeme	-0.006	0.027	0.045	0.046	0.037

(c) Accuracy (MLP Probes)

Model	Task	0%	25%	50%	75%	100%
Goldfish French (French)	Inflection	0.932	0.972	0.980	0.979	0.971
	Lexeme	0.947	0.949	0.916	0.829	0.696
Qwen2.5-1.5B (French)	Inflection	0.789	0.956	0.965	0.960	0.929
	Lexeme	0.536	0.910	0.845	0.788	0.360
Qwen2.5-1.5B-Instruct (French)	Inflection	0.791	0.954	0.962	0.959	0.929
	Lexeme	0.537	0.911	0.835	0.798	0.535
Qwen2.5-7B (French)	Inflection	0.791	0.971	0.971	0.968	0.943
	Lexeme	0.533	0.953	0.862	0.830	0.461
Qwen2.5-7B-Instruct (French)	Inflection	0.791	0.968	0.969	0.965	0.939
	Lexeme	0.534	0.949	0.851	0.823	0.467
mT5-Base (French)	Inflection	0.851	0.962	0.975	0.967	0.969
	Lexeme	0.654	0.785	0.698	0.633	0.665

(d) Selectivity (MLP Probes)

Model	Task	0%	25%	50%	75%	100%
Goldfish French (French)	Inflection	0.131	0.289	0.372	0.443	0.486
	Lexeme	-0.016	0.006	0.032	0.072	0.084
Qwen2.5-1.5B (French)	Inflection	0.236	0.260	0.402	0.405	0.548
	Lexeme	0.006	0.025	0.046	0.056	0.043
Qwen2.5-1.5B-Instruct (French)	Inflection	0.235	0.263	0.411	0.410	0.552
	Lexeme	0.002	0.030	0.048	0.055	0.064
Qwen2.5-7B (French)	Inflection	0.227	0.198	0.394	0.415	0.516
	Lexeme	-0.001	0.025	0.065	0.070	0.027
Qwen2.5-7B-Instruct (French)	Inflection	0.229	0.205	0.407	0.426	0.514
	Lexeme	0.000	0.028	0.072	0.070	0.037
mT5-Base (French)	Inflection	0.127	0.190	0.321	0.404	0.388
	Lexeme	-0.020	-0.036	-0.015	-0.000	-0.000

Table 9: Probing Results for German

(a) Accuracy (Linear Probes)

Model	Task	0%	25%	50%	75%	100%
Goldfish German (German)	Inflection	0.911	0.946	0.961	0.961	0.952
	Lexeme	0.886	0.831	0.707	0.627	0.569
Qwen2.5-1.5B (German)	Inflection	0.744	0.929	0.931	0.930	0.911
	Lexeme	0.479	0.865	0.707	0.690	0.569
Qwen2.5-1.5B-Instruct (German)	Inflection	0.745	0.928	0.929	0.929	0.912
	Lexeme	0.479	0.862	0.694	0.686	0.582
Qwen2.5-7B (German)	Inflection	0.744	0.949	0.946	0.950	0.935
	Lexeme	0.480	0.942	0.811	0.764	0.651
Qwen2.5-7B-Instruct (German)	Inflection	0.760	0.958	0.954	0.958	0.938
	Lexeme	0.480	0.943	0.801	0.757	0.646
mT5-Base (German)	Inflection	0.811	0.942	0.954	0.956	0.916
	Lexeme	0.650	0.796	0.656	0.574	0.543

(b) Selectivity (Linear Probes)

Model	Task	0%	25%	50%	75%	100%
Goldfish German (German)	Inflection	0.418	0.503	0.593	0.622	0.645
	Lexeme	-0.001	0.057	0.088	0.088	0.069
Qwen2.5-1.5B (German)	Inflection	0.289	0.446	0.577	0.582	0.599
	Lexeme	0.009	0.084	0.082	0.096	0.065
Qwen2.5-1.5B-Instruct (German)	Inflection	0.289	0.450	0.577	0.583	0.602
	Lexeme	0.009	0.082	0.082	0.098	0.069
Qwen2.5-7B (German)	Inflection	0.286	0.357	0.546	0.574	0.597
	Lexeme	0.009	0.065	0.104	0.113	0.085
Qwen2.5-7B-Instruct (German)	Inflection	0.228	0.210	0.468	0.509	0.530
	Lexeme	0.009	0.067	0.105	0.111	0.084
mT5-Base (German)	Inflection	0.251	0.371	0.494	0.560	0.529
	Lexeme	0.000	0.012	0.023	0.043	0.033

(c) Accuracy (MLP Probes)

Model	Task	0%	25%	50%	75%	100%
Goldfish German (German)	Inflection	0.923	0.955	0.969	0.969	0.960
	Lexeme	0.902	0.876	0.794	0.657	0.511
Qwen2.5-1.5B (German)	Inflection	0.741	0.943	0.944	0.942	0.910
	Lexeme	0.473	0.869	0.763	0.682	0.292
Qwen2.5-1.5B-Instruct (German)	Inflection	0.741	0.943	0.943	0.941	0.910
	Lexeme	0.474	0.870	0.753	0.688	0.300
Qwen2.5-7B (German)	Inflection	0.740	0.956	0.954	0.956	0.935
	Lexeme	0.471	0.943	0.820	0.746	0.383
Qwen2.5-7B-Instruct (German)	Inflection	0.758	0.962	0.959	0.961	0.935
	Lexeme	0.471	0.943	0.810	0.749	0.397
mT5-Base (German)	Inflection	0.820	0.956	0.954	0.952	0.939
	Lexeme	0.641	0.710	0.563	0.486	0.530

(d) Selectivity (MLP Probes)

Model	Task	0%	25%	50%	75%	100%
Goldfish German (German)	Inflection	0.229	0.350	0.457	0.523	0.585
	Lexeme	-0.021	0.017	0.051	0.084	0.082
Qwen2.5-1.5B (German)	Inflection	0.292	0.292	0.457	0.492	0.604
	Lexeme	0.008	0.022	0.054	0.060	0.035
Qwen2.5-1.5B-Instruct (German)	Inflection	0.291	0.295	0.472	0.488	0.600
	Lexeme	0.009	0.023	0.056	0.063	0.032
Qwen2.5-7B (German)	Inflection	0.288	0.214	0.455	0.493	0.596
	Lexeme	0.007	0.011	0.066	0.070	0.046
Qwen2.5-7B-Instruct (German)	Inflection	0.227	0.111	0.382	0.424	0.532
	Lexeme	0.008	0.015	0.073	0.077	0.049
mT5-Base (German)	Inflection	0.160	0.253	0.405	0.475	0.462
	Lexeme	-0.012	-0.037	0.000	0.023	0.012

Table 10: Probing Results for Russian

(a) Accuracy (Linear Probes)

Model	Task	0%	25%	50%	75%	100%
Goldfish Russian (Russian)	Inflection	0.932	0.952	0.975	0.968	0.950
	Lexeme	0.896	0.854	0.758	0.710	0.631
Qwen2.5-1.5B (Russian)	Inflection	0.850	0.966	0.966	0.962	0.933
	Lexeme	0.315	0.896	0.739	0.720	0.598
Qwen2.5-1.5B-Instruct (Russian)	Inflection	0.850	0.965	0.964	0.960	0.932
	Lexeme	0.315	0.893	0.725	0.714	0.600
Qwen2.5-7B (Russian)	Inflection	0.850	0.977	0.976	0.974	0.954
	Lexeme	0.315	0.960	0.834	0.798	0.696
Qwen2.5-7B-Instruct (Russian)	Inflection	0.858	0.977	0.974	0.980	0.953
	Lexeme	0.315	0.959	0.821	0.785	0.680
mT5-Base (Russian)	Inflection	0.882	0.944	0.974	0.971	0.952
	Lexeme	0.480	0.766	0.666	0.570	0.515

(b) Selectivity (Linear Probes)

Model	Task	0%	25%	50%	75%	100%
Goldfish Russian (Russian)	Inflection	0.505	0.568	0.663	0.675	0.688
	Lexeme	0.024	0.115	0.157	0.175	0.170
Qwen2.5-1.5B (Russian)	Inflection	0.518	0.576	0.679	0.661	0.665
	Lexeme	0.012	0.190	0.187	0.202	0.153
Qwen2.5-1.5B-Instruct (Russian)	Inflection	0.518	0.582	0.685	0.664	0.666
	Lexeme	0.012	0.191	0.190	0.205	0.152
Qwen2.5-7B (Russian)	Inflection	0.517	0.504	0.670	0.671	0.658
	Lexeme	0.011	0.165	0.218	0.222	0.183
Qwen2.5-7B-Instruct (Russian)	Inflection	0.431	0.332	0.581	0.594	0.593
	Lexeme	0.011	0.167	0.221	0.222	0.181
mT5-Base (Russian)	Inflection	0.388	0.418	0.548	0.595	0.605
	Lexeme	0.004	0.088	0.092	0.099	0.092

(c) Accuracy (MLP Probes)

Model	Task	0%	25%	50%	75%	100%
Goldfish Russian (Russian)	Inflection	0.944	0.966	0.982	0.977	0.959
	Lexeme	0.896	0.878	0.814	0.732	0.582
Qwen2.5-1.5B (Russian)	Inflection	0.848	0.972	0.971	0.969	0.924
	Lexeme	0.302	0.874	0.768	0.690	0.281
Qwen2.5-1.5B-Instruct (Russian)	Inflection	0.848	0.971	0.970	0.967	0.927
	Lexeme	0.302	0.870	0.760	0.692	0.282
Qwen2.5-7B (Russian)	Inflection	0.850	0.981	0.981	0.977	0.940
	Lexeme	0.312	0.960	0.838	0.770	0.361
Qwen2.5-7B-Instruct (Russian)	Inflection	0.857	0.976	0.976	0.978	0.935
	Lexeme	0.308	0.958	0.828	0.765	0.371
mT5-Base (Russian)	Inflection	0.883	0.956	0.978	0.974	0.971
	Lexeme	0.448	0.571	0.470	0.397	0.437

(d) Selectivity (MLP Probes)

Model	Task	0%	25%	50%	75%	100%
Goldfish Russian (Russian)	Inflection	0.322	0.466	0.557	0.604	0.642
	Lexeme	-0.007	0.049	0.120	0.203	0.201
Qwen2.5-1.5B (Russian)	Inflection	0.524	0.451	0.575	0.594	0.662
	Lexeme	0.004	0.080	0.122	0.162	0.108
Qwen2.5-1.5B-Instruct (Russian)	Inflection	0.523	0.457	0.589	0.594	0.660
	Lexeme	0.004	0.085	0.133	0.166	0.101
Qwen2.5-7B (Russian)	Inflection	0.526	0.376	0.591	0.604	0.652
	Lexeme	0.011	0.062	0.175	0.183	0.123
Qwen2.5-7B-Instruct (Russian)	Inflection	0.432	0.211	0.493	0.512	0.583
	Lexeme	0.008	0.065	0.184	0.193	0.125
mT5-Base (Russian)	Inflection	0.351	0.335	0.497	0.547	0.557
	Lexeme	-0.016	-0.016	0.023	0.035	0.042

Table 11: Probing Results for Turkish

(a) Accuracy (Linear Probes)

Model	Task	0%	25%	50%	75%	100%
Goldfish Turkish (Turkish)	Inflection	0.907	0.930	0.925	0.913	0.903
	Lexeme	0.978	0.973	0.968	0.921	0.614
Qwen2.5-1.5B (Turkish)	Inflection	0.719	0.869	0.847	0.849	0.831
	Lexeme	0.530	0.959	0.868	0.815	0.796
Qwen2.5-1.5B-Instruct (Turkish)	Inflection	0.719	0.869	0.838	0.846	0.827
	Lexeme	0.530	0.961	0.852	0.804	0.786
Qwen2.5-7B (Turkish)	Inflection	0.718	0.917	0.889	0.879	0.839
	Lexeme	0.531	0.974	0.878	0.839	0.777
Qwen2.5-7B-Instruct (Turkish)	Inflection	0.718	0.911	0.875	0.874	0.836
	Lexeme	0.531	0.975	0.854	0.803	0.731
mT5-Base (Turkish)	Inflection	0.913	0.972	0.931	0.908	0.884
	Lexeme	0.792	0.952	0.922	0.819	0.785

(b) Selectivity (Linear Probes)

Model	Task	0%	25%	50%	75%	100%
Goldfish Turkish (Turkish)	Inflection	0.345	0.407	0.491	0.492	0.500
	Lexeme	-0.002	0.008	0.074	0.089	0.144
Qwen2.5-1.5B (Turkish)	Inflection	0.277	0.323	0.452	0.455	0.411
	Lexeme	0.013	0.001	0.000	-0.014	0.008
Qwen2.5-1.5B-Instruct (Turkish)	Inflection	0.277	0.319	0.447	0.452	0.416
	Lexeme	0.013	0.003	0.004	-0.009	0.009
Qwen2.5-7B (Turkish)	Inflection	0.275	0.293	0.472	0.462	0.417
	Lexeme	0.014	-0.002	0.003	-0.010	-0.021
Qwen2.5-7B-Instruct (Turkish)	Inflection	0.276	0.291	0.463	0.497	0.445
	Lexeme	0.014	0.003	-0.003	-0.017	-0.037
mT5-Base (Turkish)	Inflection	0.071	0.165	0.261	0.331	0.366
	Lexeme	0.008	0.013	0.042	0.035	0.057

(c) Accuracy (MLP Probes)

Model	Task	0%	25%	50%	75%	100%
Goldfish Turkish (Turkish)	Inflection	0.911	0.918	0.916	0.899	0.887
	Lexeme	0.601	0.536	0.459	0.418	0.360
Qwen2.5-1.5B (Turkish)	Inflection	0.713	0.854	0.823	0.829	0.760
	Lexeme	0.459	0.500	0.369	0.325	0.232
Qwen2.5-1.5B-Instruct (Turkish)	Inflection	0.712	0.857	0.831	0.817	0.760
	Lexeme	0.462	0.491	0.367	0.333	0.233
Qwen2.5-7B (Turkish)	Inflection	0.713	0.923	0.902	0.900	0.828
	Lexeme	0.519	0.805	0.639	0.525	0.441
Qwen2.5-7B-Instruct (Turkish)	Inflection	0.717	0.914	0.900	0.895	0.820
	Lexeme	0.521	0.797	0.615	0.523	0.383
mT5-Base (Turkish)	Inflection	0.884	0.915	0.875	0.836	0.839
	Lexeme	0.503	0.395	0.300	0.257	0.312

(d) Selectivity (MLP Probes)

Model	Task	0%	25%	50%	75%	100%
Goldfish Turkish (Turkish)	Inflection	0.333	0.449	0.499	0.488	0.496
	Lexeme	0.175	0.185	0.142	0.138	0.125
Qwen2.5-1.5B (Turkish)	Inflection	0.299	0.355	0.438	0.500	0.432
	Lexeme	-0.001	0.045	0.093	0.049	0.045
Qwen2.5-1.5B-Instruct (Turkish)	Inflection	0.303	0.350	0.447	0.447	0.432
	Lexeme	0.001	0.042	0.104	0.065	-0.078
Qwen2.5-7B (Turkish)	Inflection	0.297	0.299	0.422	0.473	0.442
	Lexeme	0.007	0.084	0.128	0.105	0.065
Qwen2.5-7B-Instruct (Turkish)	Inflection	0.303	0.297	0.437	0.492	0.432
	Lexeme	0.012	0.087	0.147	0.103	0.061
mT5-Base (Turkish)	Inflection	0.120	0.301	0.343	0.355	0.368
	Lexeme	0.047	0.094	0.109	0.097	0.106

H Dataset Statistics

This section provides statistics and visualizations for the datasets and models used in our experiments across all six languages. Only words containing alphabetic characters and apostrophes were considered.

Language	Total Words	Unique Lemmas	Unique Forms	Inflection Types	Sentences	Avg. Length
English	54,816	7,848	11,720	8	8,415	6.5
Chinese	44,166	11,184	11,237	4	7,892	5.8
German	84,710	24,140	31,890	9	9,234	7.3
French	115,847	13,804	24,485	6	8,765	6.6
Russian	193,320	20,943	59,830	8	10,234	7.1
Turkish	20,881	3,776	11,680	7	6,789	6.4

Table 12: Dataset statistics across all six languages. Russian has the largest dataset and the highest number of unique forms, reflecting its rich inflectional morphology. Turkish has the fewest total words and lemmas, while Chinese has the fewest inflection types.

H.1 English Dataset Details

For the English GUM corpus specifically, the data covers three main syntactic categories: nouns (49.5%), verbs (31.2%), and adjectives (19.4%).

Table 13a shows the distribution of word categories in the English dataset, and Table 13b presents the distribution of inflection categories.

Category	Count	%
Noun	27111	49.5
Verb	17093	31.2
Adjective	10612	19.4

(a) Word categories

Inflection	Count	%
Singular	19830	36.2
Base	10076	18.4
Positive	9926	18.1
Plural	7281	13.3
Past	5604	10.2
3rd Person	1413	2.6
Comparative	403	0.7
Superlative	283	0.5

(b) Inflection categories

Metric	Value
Avg. Words	6.5
Median Words	5
Min. Words	1
Max. Words	40

(c) Sentence length stats

Table 13: Distribution statistics for the English dataset. Table (a) shows syntactic categories, (b) details inflection types, and (c) provides sentence length heuristics.

H.2 Tokenization Statistics

Model	Tokenizer Type
`BERT Base/Large`	WordPiece
`DeBERTa V3 Large`	SentencePiece
`GPT-2 variants`	BPE
`Pythia variants`	BPE
`OLMo 2 variants`	BPE (`tiktoken`)
`Gemma 2 variants`	SentencePiece
`Qwen 2.5 variants`	Byte-level BPE
`Llama 3.1 variants`	BPE (`tiktoken`)

Table 14: Tokenization strategies used by different model families. BPE means byte-pair encoding.

An important consideration for our analysis is how different models tokenize the words in our dataset. Table 15 shows tokenization statistics across the models we analyze. Encoder-only models

like BERT and DeBERTa tend to split words into more tokens than decoder-only models like GPT-2 and Qwen2, which may affect how information is encoded across layers.

Model	Avg. tokens per word	Med. tokens per word	Max tokens per word	Percent multitoken
BERT variants	1.11	1.0	6.0	6.95
DeBERTa-v3-large	1.03	1.0	4.0	2.2
GPT-2 variants	1.52	1.0	5.0	42.25
Pythia-6.9B variants	1.48	1.0	5.0	39.1
OLMo2-7B variants	1.43	1.0	4.0	35.9
Gemma2-2B variants	1.19	1.0	4.0	16.55
Qwen2.5-1.5B variants	1.43	1.0	4.0	35.9
Llama-3.1-8B variants	1.43	1.0	4.0	35.85

Table 15: Tokenization statistics across different models (English only). Most models have an average of 1.0-1.5 tokens per word and a median of 1, indicating that most words are tokenized as a single unit. However, there is variation in the proportion of words split into multiple tokens. Decoder-only models (*e.g.*, , GPT-2, Pythia, Qwen2, LLaMA) split 35-42% of words, while BERT and DeBERTa variants split fewer words (2-7%). Maximum tokens per word range from 4 to 6 across all models.

H.3 Effects of Tokenization

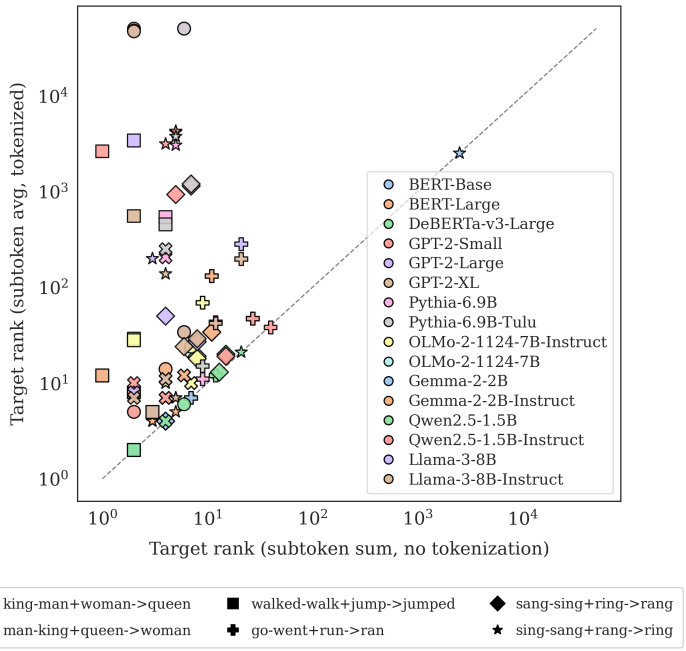

Figure 14: Effect of tokenization strategy on analogy completion rank. Each point corresponds to a model (color) and analogy (shape). The x-axis is the rank using whole-word representations. The y-axis is the rank using tokenized representations. Here, rank means the position of the expected word when all vocabulary words are sorted by similarity to the resulting embedding from vector arithmetic; lower is better. Points above the gray $y{=}x$ line mean tokenization hurts performance.

Tokenization is an essential component of language modeling. To test how tokenization influences our findings, we use analogy completion tasks in English (*e.g.*, *man:king::woman:?*) and compare two approaches: averaging subtoken embeddings after standard tokenization and summing embeddings from whole-word tokens.

For each approach, we perform vector arithmetic on word representations (*e.g.*, *king - man + woman*). We measure performance by ranking all vocabulary words by cosine similarity to the resulting

representation, and observe how highly the expected word (*e.g.*, *queen*) ranks, with a lower rank indicating better performance.

Whole-word representations markedly outperform averaged subtokens across all models (Figure 14), implying that linguistic regularities are primarily stored in whole-word embeddings rather than compositionally across subtokens. Despite tokenization effects, our classifier results show consistent patterns across models using different tokenizers (see Table 14), indicating robust encoding of lexical and morphological information.

Model	HuggingFace ID
BERT-Base	bert-base-uncased
BERT-Large	bert-large-uncased
DeBERTa-v3-Large	microsoft/deberta-v3-large
mT5-base	google/mt5-base
GPT-2-Small	openai-community/gpt2
GPT-2-Large	openai-community/gpt2-large
GPT-2-XL	openai-community/gpt2-xl
Pythia-6.9B	EleutherAI/pythia-6.9b
Pythia-6.9B-Tulu	allenai/open-instruct-pythia-6.9b-tulu
OLMo-2-1124-7B	allenai/OLMo-2-1124-7B
OLMo-2-1124-7B-Instruct	allenai/OLMo-2-1124-7B-Instruct
Gemma-2-2B	google/gemma-2-2b
Gemma-2-2B-Instruct	google/gemma-2-2b-it
Qwen2.5-1.5B	Qwen/Qwen2.5-1.5B
Qwen2.5-1.5B-Instruct	Qwen/Qwen2.5-1.5B-Instruct
Qwen2.5-7B	Qwen/Qwen2.5-7B
Qwen2.5-7B-Instruct	Qwen/Qwen2.5-7B-Instruct
Llama-3.1-8B	meta-llama/Llama-3.1-8B
Llama-3.1-8B-Instruct	meta-llama/Llama-3.1-8B-Instruct
Goldfish English	goldfish-models/goldfish_eng_latn_1000mb
Goldfish Chinese	goldfish-models/goldfish_zho_hans_1000mb
Goldfish German	goldfish-models/goldfish_deu_latn_1000mb
Goldfish French	goldfish-models/goldfish_fra_latn_1000mb
Goldfish Russian	goldfish-models/goldfish_rus_cyrl_1000mb
Goldfish Turkish	goldfish-models/goldfish_tur_latn_1000mb

Table 16: Canonical HuggingFace model IDs used to load models in our study.

I Additional Analysis

I.1 Intrinsic Dimensionality Results

Intrinsic dimensionality analyses are shown in Figure 15 and Table 17. These illustrate how compression varies across layers and between models.

Model	d_{model}	ID_{50}			ID_{70}			ID_{90}		
		First	Mid	Final	First	Mid	Final	First	Mid	Final
BERT-Base	768	123	100	88	244	212	192	461	451	446
BERT-Large	1024	138	105	85	286	226	208	567	527	554
DeBERTa-v3-Large	1024	196	133	29	377	299	113	688	635	423
GPT-2-Small	768	37	1	1	152	1	1	402	1	3
GPT-2-Large	1280	24	1	95	172	1	284	583	1	726
GPT-2-XL	1600	113	1	118	340	1	356	838	1	914
Pythia-6.9B	4096	391	1	96	865	1	517	1952	1	1925
Pythia-6.9B-Tulu	4096	390	1	244	862	1	832	1949	1	2292
OLMo-2-7B	4096	404	310	41	833	896	299	1772	2279	1550
OLMo-2-7B-Instruct	4096	404	358	111	833	974	567	1772	2361	1964
Gemma-2-2B	2304	216	8	11	505	130	70	1129	794	611
Gemma-2-2B-Instruct	2304	222	22	8	520	198	57	1153	899	572
Qwen-2.5-1.5B	1536	184	1	9	399	1	50	835	1	452
Qwen-2.5-1.5B-Instruct	1536	184	1	11	394	1	70	820	1	533
Llama-3.1-8B	4096	373	240	35	789	727	187	1722	2051	1119
Llama-3.1-8B-Instruct	4096	372	215	31	788	664	181	1722	1957	1093

Table 17: Number of principal-component axes required to reach 50% (ID_{50}), 70% (ID_{70}) and 90% (ID_{90}) explained variance in the first, middle and last layers of each model.

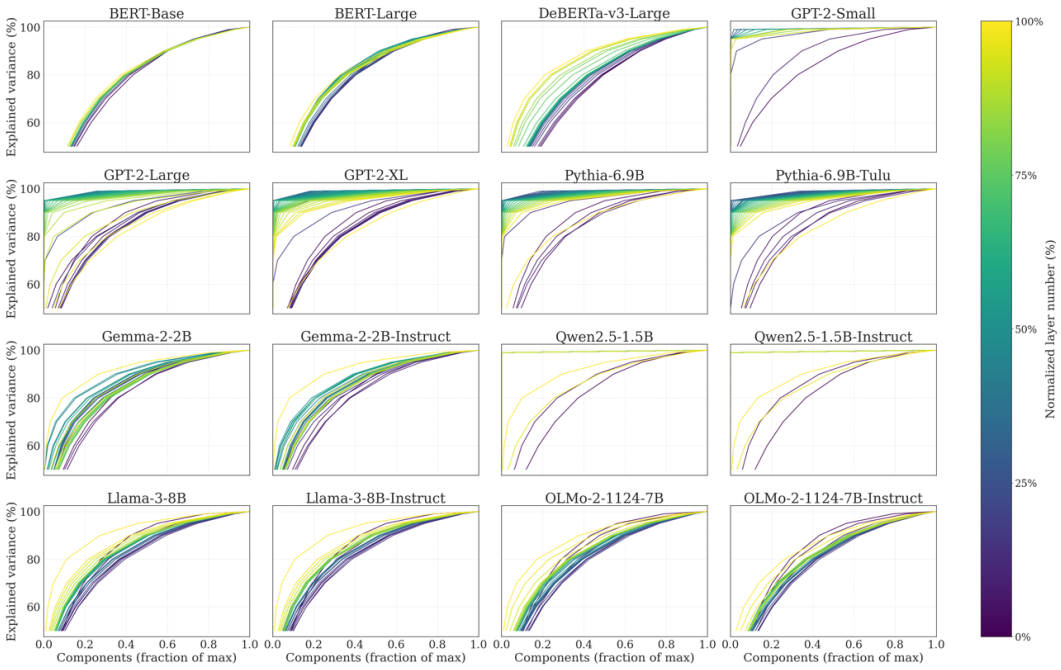

Figure 15: Intrinsic dimensionality curves for all models for English. Each subplot shows the relationship between the percentage of maximum PCA components (x-axis) and the percentage of explained variance (y-axis) across different layers. The color gradient from purple (early layers, 0%) to yellow (late layers, 100%) indicates the relative layer depth within each model. Models like `BERT`, `Gemma`, and `Llama` show similar compression patterns, while `GPT-2` variants, `Qwen` and `Pythia` exhibit opposite trends in their middle layers.

I.2 Massive Activations and Outlier Dimensions

We computed the maximum absolute activation, maximum mean (absolute value) per dimension, and maximum standard deviation per dimension across all layers for representative models to understand the low intrinsic dimensionality observed in Table Table 17.

Figures Figures 16–22 show the results. Models like `Qwen2.5-1.5B` and `GPT-2` variants show large maximum activation values. For example, `Qwen2.5-1.5B` reaches maximum absolute activations around 8000, while models like `Llama-3-8B` and `OLMo-1124-7B` show gradual increases across layers, with maximum values only reaching 30-40 in final layers.

This corresponds with the intrinsic dimensionality measurements in Table Table 17. Models with large activations in middle layers correspond to those requiring only 1-2 components to reach 50-90% explained variance at those depths. Models with gradual activation increases correspond to those requiring hundreds of components at all depths. The presence of outlier dimensions with large activations makes the representation anisotropic, with variance concentrated along a small number of directions.

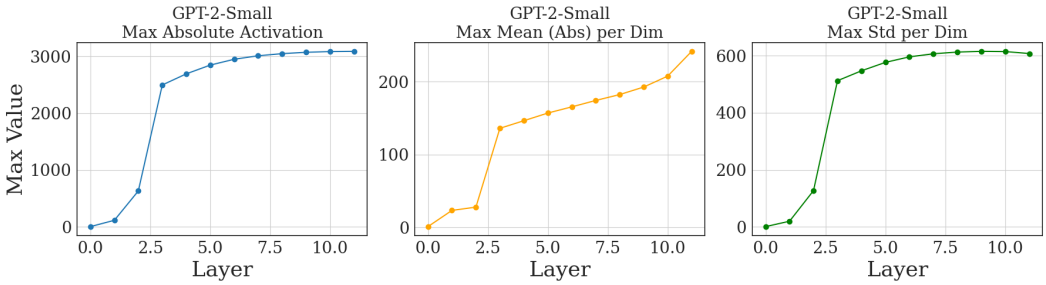

Figure 16: Activation statistics across layers for `GPT-2-Small`.

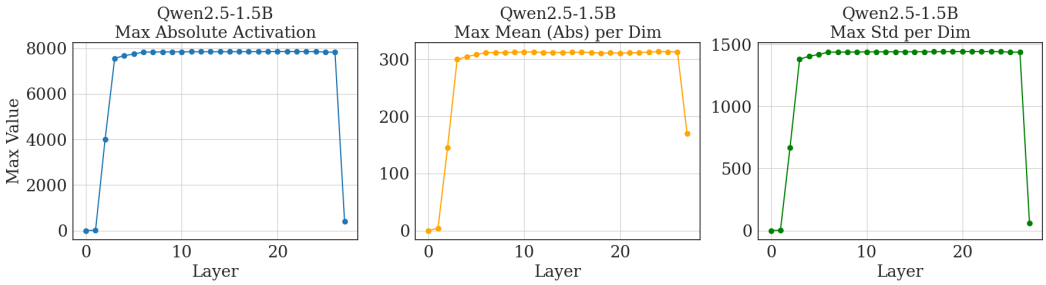

Figure 17: Activation statistics across layers for `Qwen2.5-1.5B`.

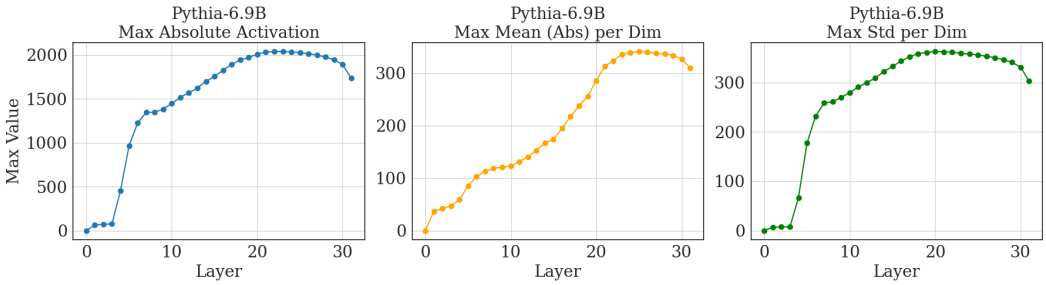

Figure 18: Activation statistics across layers for `Pythia-6.9B`.

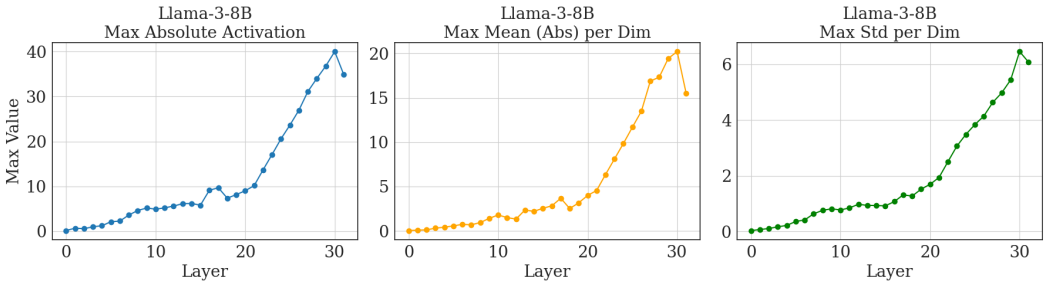

Figure 19: Activation statistics across layers for `Llama-3-8B`.

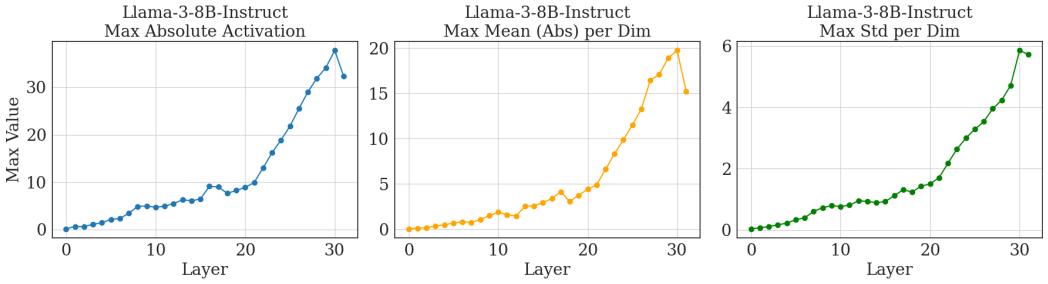

Figure 20: Activation statistics across layers for `Llama-3-8B-Instruct`.

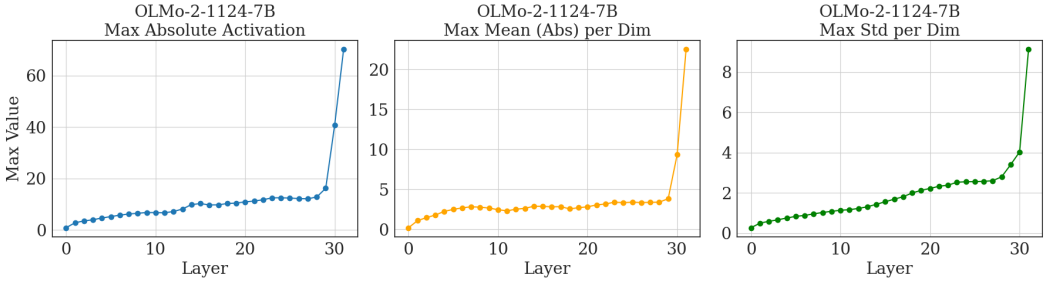

Figure 21: Activation statistics across layers for `OLMo-2-1124-7B`.

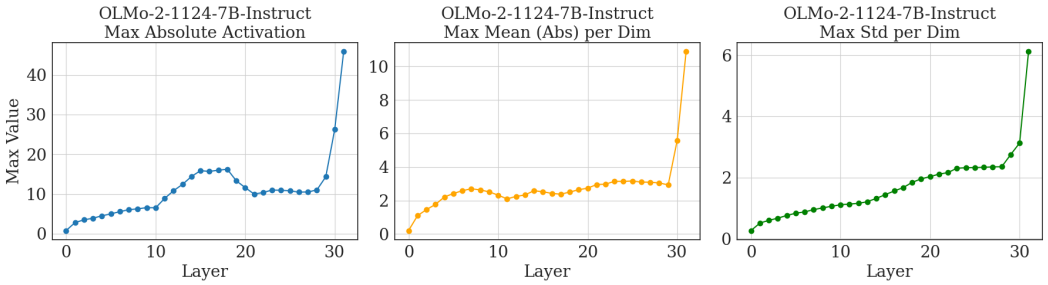

Figure 22: Activation statistics across layers for `OLMo-2-1124-7B-Instruct`.

I.3 Linear Separability Gap

Figures 23 and 24 show the linear separability gap for lemma and inflection prediction across models and layers.

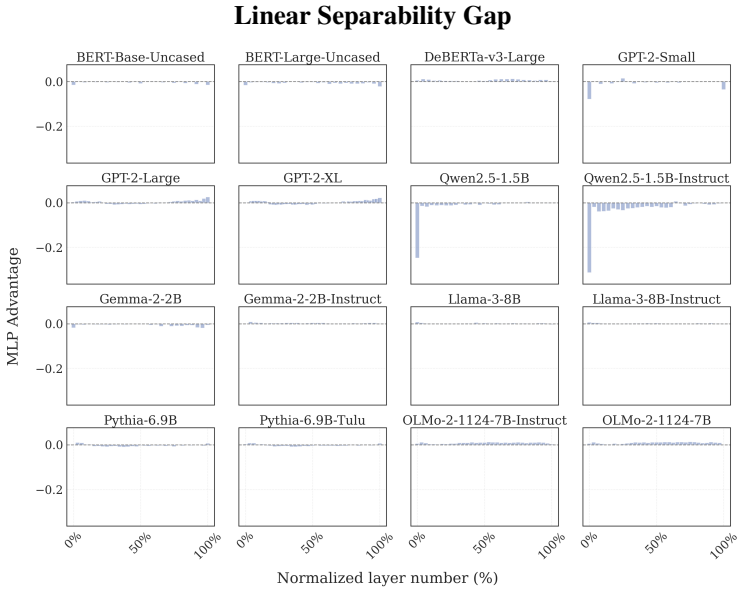

(a) Linear separability gap for inflection prediction

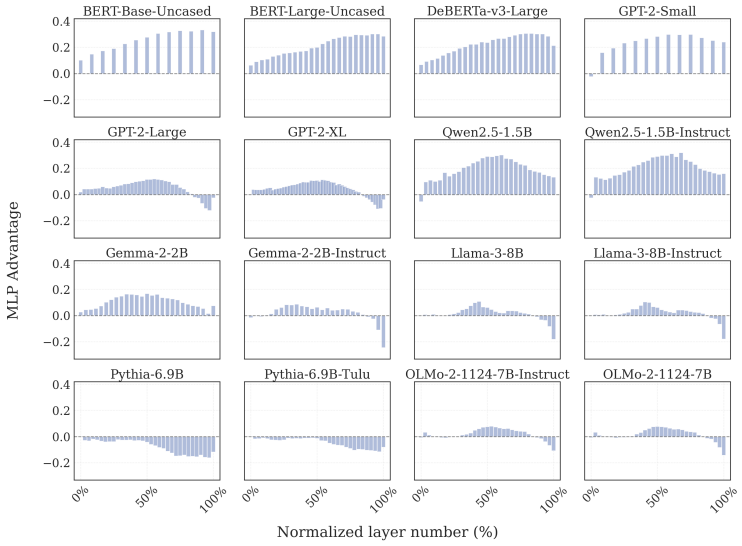

(b) Linear separability gap for lemma prediction

Figure 23: Performance advantage of MLP classifiers over linear classifiers (in percentage points) across model layers for English. The linear separability gap measures how much a non-linear transformation improves classifier performance compared to a simple linear mapping. For inflection prediction, the gap is consistently minimal (mostly within ± 0.02 percentage points) and sometimes negative, indicating that inflectional features are primarily encoded in a linear fashion throughout the network. By contrast, the linear separability gap for lemma prediction is relatively large (0.1–0.3 percentage points) and positive across most models

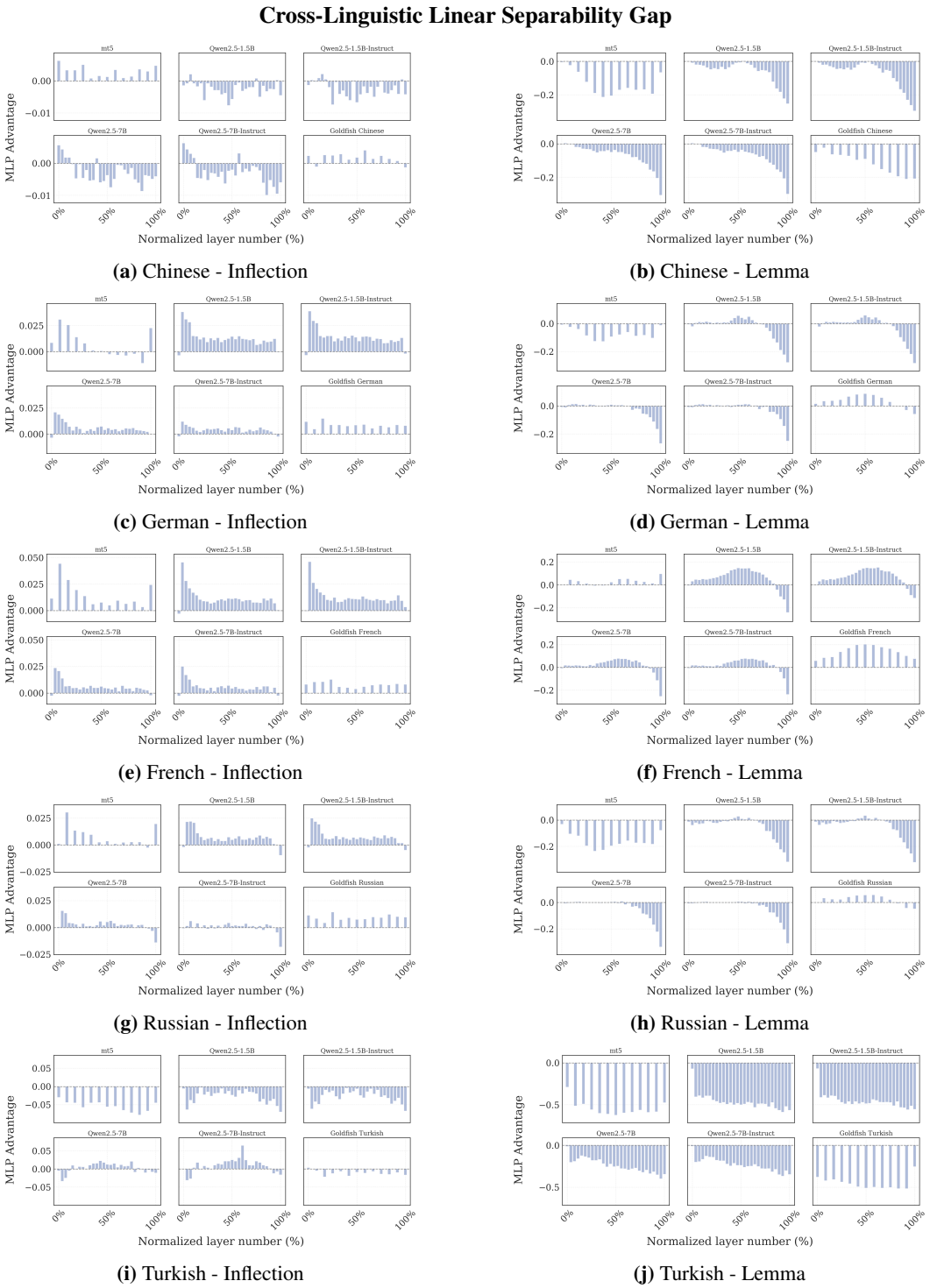

(a) Chinese - Inflection

(b) Chinese - Lemma

(c) German - Inflection

(d) German - Lemma

(e) French - Inflection

(f) French - Lemma

(g) Russian - Inflection

(h) Russian - Lemma

(i) Turkish - Inflection

(j) Turkish - Lemma

Figure 24: Cross-linguistic linear separability gap showing performance advantage of MLP classifiers over linear classifiers across model layers for five additional languages. For inflectional features, `mT5` and `Goldfish` models show slight positive gaps (indicating modest benefits from non-linear classification), while `Qwen2.5` variants show slight negative gaps (indicating linear classifiers are sufficient or superior). For lexical features, all models show negative gaps that are most pronounced in early layers, suggesting that linear regression with regularization consistently outperforms MLPs for lexical classification across all model families and languages.

I.4 Training Dynamics

See Figures 25 and 26 for probing accuracy and selectivity across pretraining checkpoints for `OLMo-2-7B` and `Pythia-6.9B`.

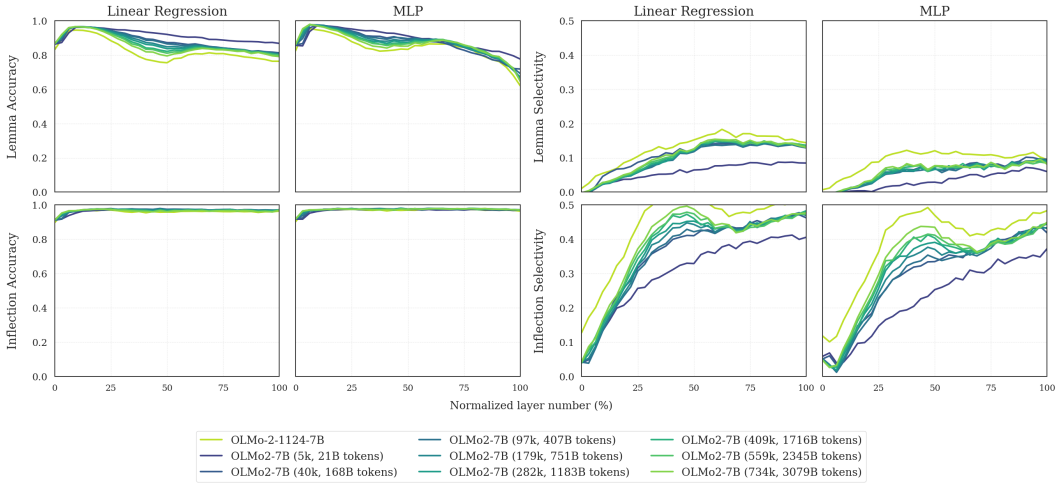

Figure 25: `OLMo-2-7B` **Training Dynamics.** Performance across pretraining checkpoints (5k–734k steps) for English. The full model is 928k steps. Checkpoints are colored from brightest (earliest) to darkest (latest). **Left:** Prediction accuracy for Lemma (top) and Inflection (bottom). Early checkpoints exhibit higher lemma accuracy than later ones, while inflectional accuracy remains flat. **Right:** Selectivity scores for the same tasks. Selectivity generally increases with model depth and training steps, particularly for inflection.

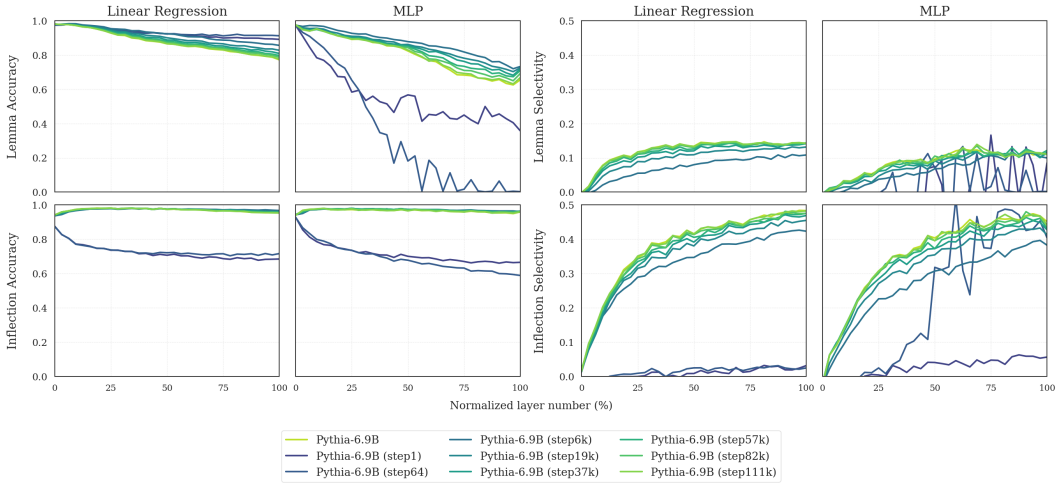

Figure 26: `Pythia-6.9B` **Training Dynamics.** Performance across pretraining checkpoints (step 1–111k) for English. The full model is 143k steps. Checkpoints are colored from brightest (earliest) to darkest (latest). **Left:** Prediction accuracy for Lemma (top) and Inflection (bottom). Lemma accuracy declines both with deeper layers and with more training, whereas inflectional accuracy stays uniformly high. **Right:** Selectivity scores for the same tasks, showing distinct separation between early and late checkpoints in the inflection task.

J Attention Head Analysis

We conducted additional experiments analyzing attention head outputs alongside residual stream representations to understand how different components of transformer models contribute to linguistic encoding.

J.1 Methodology

We averaged activations across all attention heads at each layer for `Qwen2.5-1.5B` and `Qwen2.5-1.5B-Instruct` models using the English dataset. We then trained linear regression and MLP classifiers on both attention head outputs and residual stream representations to compare their encoding patterns.

J.2 Results

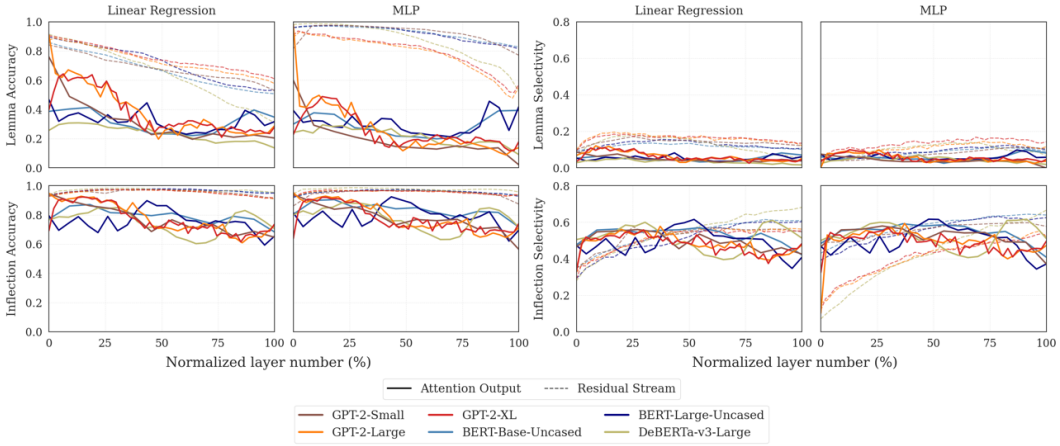

Figure 27: Combined analysis of linguistic task accuracy (left two columns) and classifier selectivity (right two columns) for attention head outputs (solid lines) versus residual stream representations (dashed lines) across BERT and GPT-2 model families. The top row corresponds to Lemma tasks, and the bottom row to Inflection tasks.

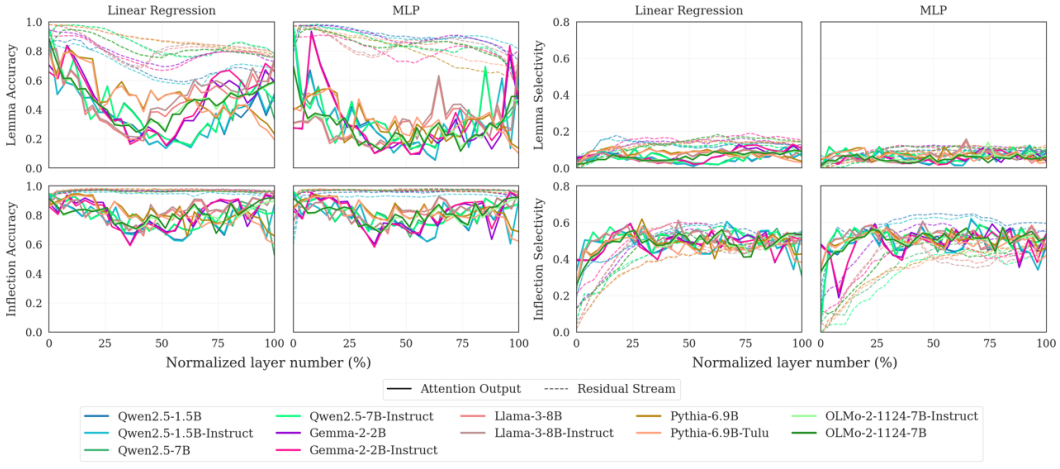

Figure 28: Combined analysis of linguistic task accuracy (left two columns) and classifier selectivity (right two columns) for attention head outputs (solid lines) versus residual stream representations (dashed lines) across contemporary model families. The top row corresponds to Lemma tasks, and the bottom row to Inflection tasks.

K Steering Vector Analysis

We conducted steering vector experiments to test whether inflectional representations can be functionally manipulated and to understand model sensitivity to activation interventions.

K.1 Methodology

For each inflectional category, we computed steering vectors as:

$$\mathbf{s}_i = \mu_i - \lambda \cdot \frac{1}{|C| - 1} \sum_{j \in C, j \neq i} \mu_j \tag{7}$$

We tested multiple values of λ (1, 5, 10, 20, 100) and measured the impact on MLP classifier performance when adding these steering vectors to existing activations for 1000 test words. We evaluated both mean probability change and prediction flip rate across all models.

K.2 Results

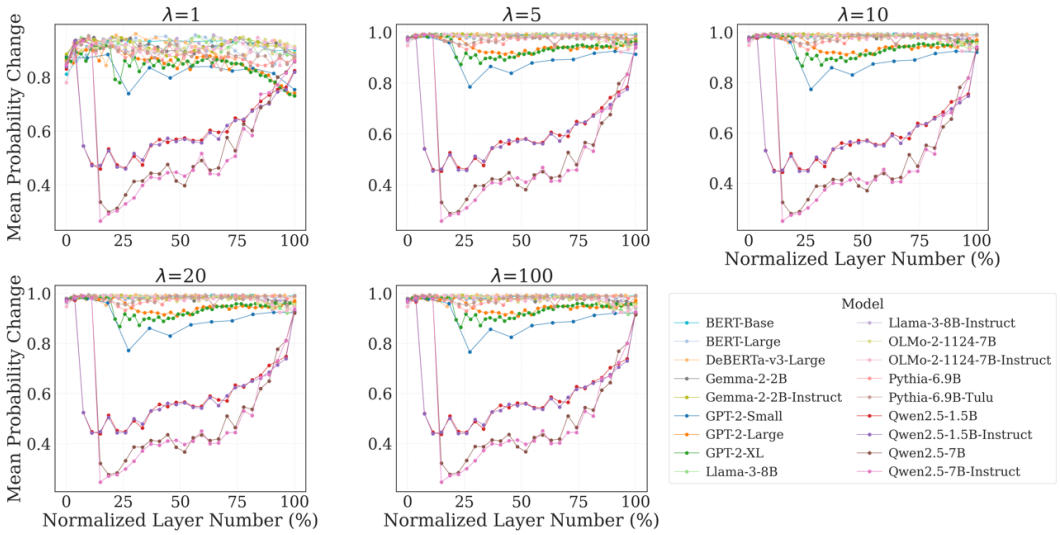

Figure 29: Mean probability change for inflection prediction when applying steering vectors across different λ values. Five panels show results for $\lambda \in \{1, 5, 10, 20, 100\}$. All models start with high effectiveness ($\approx$0.9-1.0) at layer 0. Most models maintain stable performance, but Qwen2.5 variants show pronounced sensitivity dips around 10% layer depth before recovering. Higher λ values increase steering effectiveness while preserving the overall pattern.

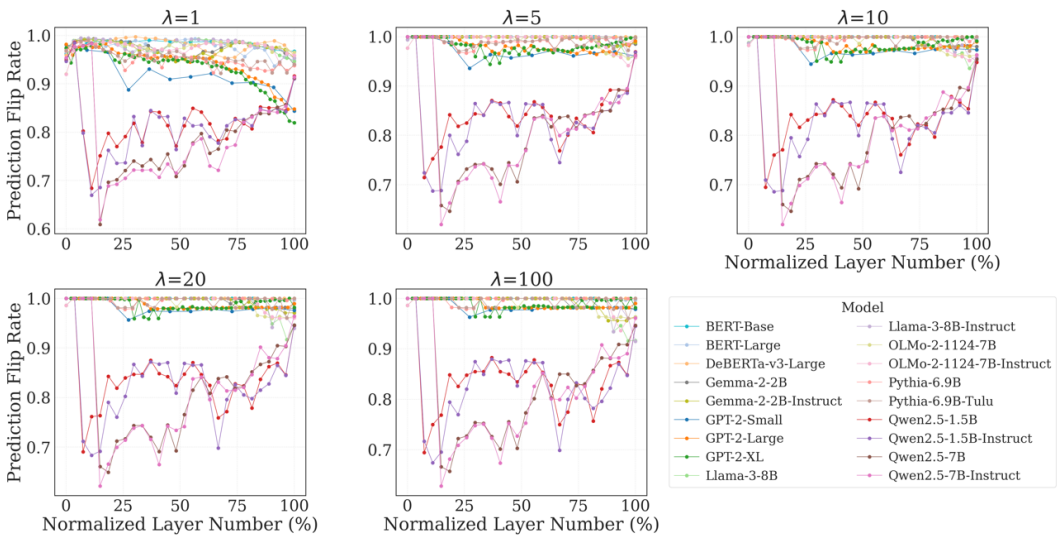

Figure 30: Prediction flip rate when applying steering vectors across different λ values. The flip rate patterns mirror the probability change results, with most models maintaining high rates (0.98-1.00) throughout all layers. Qwen2.5 variants show characteristic V-shaped dips to ≈0.60-0.70 around 10% layer depth. The consistency across λ values suggests that steering effectiveness depends more on model architecture than intervention strength.

L Classifier Error Analysis

We conducted a detailed error analysis of our classifiers to better understand their performance across different morphological features and languages. See Table 18 through Table 36 for the full results.

Model	3rd person (n=249)	Base (n=1,833)	Comparative (n=76)	Past (n=1,003)	Plural (n=1,247)	Positive (n=1,785)	Singular (n=3,587)	Superlative (n=52)
BERT-Base	0.960	0.965	0.817	0.967	0.983	0.946	0.971	0.759
BERT-Large	0.956	0.964	0.861	0.968	0.982	0.950	0.971	0.768
DeBERTa-v3-Large	0.938	0.974	0.831	0.961	0.986	0.954	0.977	0.706
GPT-2-Small	0.828	0.958	0.840	0.956	0.974	0.941	0.964	0.754
GPT-2-Large	0.812	0.958	0.826	0.951	0.975	0.936	0.967	0.792
GPT-2-XL	0.817	0.959	0.813	0.948	0.977	0.940	0.968	0.788
Pythia-6.9B	0.886	0.972	0.904	0.964	0.989	0.957	0.977	0.907
Pythia-6.9B-Tulu	0.899	0.973	0.909	0.967	0.989	0.956	0.976	0.910
OLMo-2-1124-7B	0.938	0.968	0.902	0.972	0.981	0.923	0.966	0.888
OLMo-2-1124-7B-Instruct	0.927	0.967	0.896	0.971	0.981	0.923	0.965	0.872
Gemma-2-2B	0.901	0.968	0.797	0.969	0.986	0.947	0.974	0.833
Gemma-2-2B-Instruct	0.913	0.966	0.863	0.973	0.988	0.938	0.972	0.872
Qwen2.5-1.5B	0.856	0.950	0.802	0.942	0.972	0.919	0.957	0.688
Qwen2.5-1.5B-Instruct	0.774	0.954	0.647	0.945	0.972	0.921	0.965	0.630

Table 18: Breakdown of inflection classification accuracy by morphological feature for each model using linear regression classifiers (English). Inflections are grouped by their morphological features (*e.g.*, Past, Plural, Comparative). For each group, the reported accuracy is the average of accuracies from classifiers trained at each model layer. All accuracy values are on a 0–1 scale. Comparative and superlative forms consistently show the lowest accuracy across all models, reflecting the challenges of these less frequent morphological categories.

Model	3rd person (n=249)	Base (n=1,833)	Comparative (n=76)	Past (n=1,003)	Plural (n=1,247)	Positive (n=1,785)	Singular (n=3,587)	Superlative (n=52)
BERT-Base	0.973	0.969	0.910	0.972	0.989	0.959	0.974	0.939
BERT-Large	0.967	0.970	0.910	0.973	0.988	0.961	0.975	0.931
DeBERTa-v3-Large	0.954	0.976	0.925	0.966	0.989	0.962	0.979	0.867
GPT-2-Small	0.921	0.963	0.928	0.952	0.972	0.930	0.963	0.870
GPT-2-Large	0.857	0.962	0.872	0.955	0.976	0.942	0.967	0.854
GPT-2-XL	0.921	0.963	0.928	0.952	0.972	0.930	0.963	0.870
Pythia-6.9B	0.932	0.972	0.921	0.961	0.982	0.949	0.971	0.886
Pythia-6.9B-Tulu	0.948	0.974	0.932	0.964	0.983	0.949	0.971	0.897
OLMo-2-1124-7B	0.957	0.968	0.926	0.966	0.989	0.949	0.973	0.905
OLMo-2-1124-7B-Instruct	0.939	0.967	0.903	0.967	0.988	0.949	0.973	0.873
Gemma-2-2B	0.913	0.967	0.863	0.968	0.990	0.950	0.976	0.907
Gemma-2-2B-Instruct	0.930	0.970	0.878	0.975	0.989	0.946	0.974	0.906
Qwen2.5-1.5B	0.882	0.948	0.822	0.943	0.974	0.927	0.957	0.736
Qwen2.5-1.5B-Instruct	0.808	0.953	0.697	0.947	0.974	0.930	0.965	0.682

Table 19: Breakdown of inflection classification accuracy by morphological feature for each model using Multi-Layer Perceptron (MLP) classifiers (English). Inflections are grouped by their morphological features (*e.g.*, Past, Plural, Comparative). For each group, the reported accuracy is the average of accuracies from classifiers trained at each model layer. All accuracy values are on a 0–1 scale. MLP classifiers provide modest improvements over linear regression, particularly for comparative and superlative forms, though the relative ordering across morphological features remains consistent.

Model	Noun (n=1,739)	Verb (n=641)	Adjective (n=641)	Adverb (n=23)	Pronoun (n=1)	Preposition (n=1)	Conjunction (n=1)	Interjection (n=1)	Other (n=9)
BERT-Base	0.636	0.737	0.609	0.805	0.292	0.000	0.585	0.000	0.902
BERT-Large	0.684	0.777	0.653	0.826	0.580	0.154	0.662	0.065	0.897
DeBERTa-v3-Large	0.592	0.737	0.585	0.723	0.440	0.077	0.438	0.081	0.866
GPT-2-Small	0.631	0.789	0.612	0.813	0.542	0.000	0.415	0.033	0.896
GPT-2-Large	0.691	0.810	0.688	0.847	0.853	0.174	0.267	0.115	0.912
GPT-2-XL	0.713	0.827	0.708	0.847	0.724	0.222	0.311	0.241	0.899
Pythia-6.9B	0.856	0.926	0.836	0.926	0.938	0.443	0.566	0.488	0.934
Pythia-6.9B-Tulu	0.864	0.930	0.843	0.930	0.923	0.514	0.651	0.476	0.936
OLMo-2-1124-7B	0.798	0.875	0.794	0.913	0.697	0.339	0.363	0.495	0.913
OLMo-2-1124-7B-Instruct	0.798	0.868	0.792	0.902	0.606	0.339	0.331	0.495	0.910
Gemma-2-2B	0.757	0.869	0.736	0.876	0.667	0.179	0.205	0.288	0.891
Gemma-2-2B-Instruct	0.749	0.844	0.742	0.872	0.620	0.137	0.152	0.247	0.912
Qwen2.5-1.5B	0.652	0.801	0.650	0.828	0.526	0.082	0.223	0.068	0.867
Qwen2.5-1.5B-Instruct	0.642	0.800	0.632	0.831	0.544	0.082	0.245	0.068	0.877
Llama-3.1-8B	0.776	0.882	0.771	0.887	0.831	0.286	0.396	0.321	0.911
Llama-3.1-8B-Instruct	0.796	0.892	0.788	0.896	0.908	0.300	0.443	0.357	0.917

Table 20: Breakdown of lemma classification accuracy by Part of Speech (POS) for each model using linear regression classifiers (English). Lemmas are grouped by their POS tags (*e.g.*, Noun, Verb, Adjective). For each group, the reported accuracy is the average of accuracies from classifiers trained at each model layer. All accuracy values are on a 0–1 scale. Performance varies significantly with frequency: frequent categories like nouns and verbs achieve higher accuracy, while infrequent categories like pronouns and prepositions show lower performance due to limited training examples.

Model	Noun (n=1,739)	Verb (n=641)	Adjective (n=641)	Adverb (n=23)	Pronoun (n=1)	Preposition (n=1)	Conjunction (n=1)	Interjection (n=1)	Other (n=9)
BERT-Base	0.775	0.831	0.748	0.873	0.458	0.125	0.756	0.267	0.898
BERT-Large	0.813	0.863	0.785	0.884	0.540	0.231	0.725	0.323	0.897
DeBERTa-v3-Large	0.689	0.803	0.682	0.802	0.700	0.115	0.662	0.242	0.861
GPT-2-Small	0.678	0.792	0.665	0.765	0.042	0.000	0.610	0.000	0.830
GPT-2-Large	0.754	0.837	0.755	0.827	0.347	0.188	0.596	0.385	0.871
GPT-2-XL	0.774	0.844	0.771	0.827	0.561	0.232	0.561	0.431	0.860
Pythia-6.9B	0.774	0.856	0.768	0.862	0.554	0.229	0.528	0.310	0.868
Pythia-6.9B-Tulu	0.818	0.880	0.803	0.887	0.554	0.343	0.613	0.381	0.889
OLMo-2-1124-7B	0.818	0.877	0.828	0.896	0.727	0.290	0.734	0.505	0.885
OLMo-2-1124-7B-Instruct	0.822	0.874	0.829	0.897	0.667	0.306	0.750	0.473	0.886
Gemma-2-2B	0.763	0.860	0.763	0.881	0.574	0.125	0.443	0.182	0.880
Gemma-2-2B-Instruct	0.777	0.846	0.785	0.882	0.580	0.137	0.400	0.299	0.875
Qwen2.5-1.5B	0.747	0.838	0.742	0.811	0.228	0.131	0.628	0.164	0.857
Qwen2.5-1.5B-Instruct	0.749	0.840	0.738	0.818	0.211	0.098	0.564	0.123	0.860
Llama-3.1-8B	0.798	0.879	0.807	0.886	0.800	0.214	0.679	0.393	0.882
Llama-3.1-8B-Instruct	0.824	0.893	0.826	0.895	0.831	0.257	0.689	0.429	0.887

Table 21: Breakdown of lemma classification accuracy by Part of Speech (POS) for each model using Multi-Layer Perceptron (MLP) classifiers (English). Lemmas are grouped by their POS tags (*e.g.*, Noun, Verb, Adjective). For each group, the reported accuracy is the average of accuracies from classifiers trained at each model layer. All accuracy values are on a 0–1 scale. MLP classifiers provide consistent improvements over linear regression across all POS categories, though the frequency-dependent performance patterns persist.

Model	Linear Regression				MLP			
	Positive (n=300)	Base (n=2,074)	Plural (n=3)	Singular (n=3,947)	Positive (n=300)	Base (n=2,074)	Plural (n=3)	Singular (n=3,947)
mT5-Base	0.739	0.913	0.436	0.962	0.783	0.919	0.231	0.961
Qwen2.5-1.5B	0.785	0.929	0.034	0.969	0.801	0.924	0.092	0.967
Qwen2.5-1.5B-Instruct	0.779	0.925	0.034	0.964	0.803	0.923	0.057	0.967
Qwen2.5-7B	0.824	0.937	0.310	0.970	0.828	0.929	0.310	0.969
Qwen2.5-7B-Instruct	0.819	0.936	0.299	0.970	0.823	0.928	0.276	0.969
Goldfish Chinese	0.793	0.912	0.000	0.958	0.816	0.915	0.000	0.957

Table 22: Breakdown of inflection classification accuracy for each model by inflection type using Linear Regression and Multi-Layer Perceptron (MLP) classifiers (Chinese). Accuracies are calculated over all examples for a given group across all layers. Counts (n) are derived from a single representative layer for each group. All accuracy values are on a 0–1 scale.

Model	Noun (n=1,179)	Verb (n=564)	Adjective (n=108)	Adverb (n=22)	Preposition (n=20)	Other (n=50)
mT5-Base	0.838	0.828	0.786	0.762	0.920	0.726
Qwen2.5-1.5B	0.810	0.797	0.746	0.715	0.872	0.699
Qwen2.5-1.5B-Instruct	0.813	0.799	0.748	0.713	0.873	0.700
Qwen2.5-7B	0.887	0.882	0.846	0.847	0.915	0.817
Qwen2.5-7B-Instruct	0.886	0.877	0.843	0.835	0.913	0.811
Goldfish Chinese	0.883	0.878	0.845	0.875	0.954	0.858

Table 23: Breakdown of lemma classification accuracy by Part of Speech (POS) for each model, using Linear Regression classifiers (Chinese). Lemmas are grouped by their POS tags (*e.g.*, , Noun, Verb, Adjective). Accuracies are calculated over all examples for a given group across all layers. Counts (n) are derived from a single representative layer for each group. All accuracy values are on a 0–1 scale.

Model	Noun (n=1,179)	Verb (n=564)	Adjective (n=108)	Adverb (n=22)	Preposition (n=20)	Other (n=50)
mT5-Base	0.698	0.712	0.564	0.571	0.884	0.569
Qwen2.5-1.5B	0.748	0.761	0.658	0.668	0.826	0.669
Qwen2.5-1.5B-Instruct	0.735	0.745	0.643	0.643	0.814	0.655
Qwen2.5-7B	0.815	0.826	0.749	0.745	0.848	0.750
Qwen2.5-7B-Instruct	0.815	0.822	0.747	0.734	0.845	0.744
Goldfish Chinese	0.766	0.771	0.647	0.621	0.912	0.682

Table 24: Breakdown of lemma classification accuracy by Part of Speech (POS) for each model, using Multi-Layer Perceptron (MLP) classifiers (Chinese). Lemmas are grouped by their POS tags (*e.g.*, , Noun, Verb, Adjective). Accuracies are calculated over all examples for a given group across all layers. Counts (n) are derived from a single representative layer for each group. All accuracy values are on a 0–1 scale.

Model	Base (n=417)	3rd person (n=517)	Positive (n=1,720)	Past (n=839)	Plural (n=1,076)	Superlative (n=52)	Singular (n=3,197)	Comparative (n=141)
mT5-Base	0.908	0.941	0.940	0.960	0.882	0.572	0.962	0.636
Qwen2.5-1.5B	0.849	0.889	0.922	0.914	0.888	0.657	0.953	0.796
Qwen2.5-1.5B-Instruct	0.844	0.887	0.922	0.910	0.889	0.659	0.952	0.795
Qwen2.5-7B	0.892	0.922	0.939	0.947	0.909	0.826	0.962	0.878
Qwen2.5-7B-Instruct	0.915	0.934	0.945	0.962	0.924	0.866	0.968	0.909
Goldfish German	0.938	0.941	0.955	0.979	0.916	0.542	0.968	0.708

Table 25: Breakdown of inflection classification accuracy for each model by inflection type using Linear Regression classifiers (German). Accuracies are calculated over all examples for a given group across all layers. Counts (n) are derived from a single representative layer for each group. All accuracy values are on a 0–1 scale.

Model	Base (n=417)	3rd person (n=517)	Positive (n=1,720)	Past (n=839)	Plural (n=1,076)	Superlative (n=52)	Singular (n=3,197)	Comparative (n=141)
mT5-Base	0.921	0.945	0.948	0.959	0.884	0.723	0.967	0.770
Qwen2.5-1.5B	0.890	0.915	0.930	0.940	0.897	0.831	0.958	0.892
Qwen2.5-1.5B-Instruct	0.888	0.914	0.930	0.938	0.898	0.825	0.957	0.897
Qwen2.5-7B	0.912	0.932	0.944	0.956	0.913	0.868	0.964	0.924
Qwen2.5-7B-Instruct	0.925	0.941	0.950	0.966	0.928	0.901	0.970	0.936
Goldfish German	0.947	0.957	0.964	0.978	0.923	0.817	0.970	0.896

Table 26: Breakdown of inflection classification accuracy for each model by inflection type using Multi-Layer Perceptron (MLP) classifiers (German). Accuracies are calculated over all examples for a given group across all layers. Counts (n) are derived from a single representative layer for each group. All accuracy values are on a 0–1 scale.

Model	Linear Regression				MLP			
	Noun (n=1,262)	Verb (n=395)	Adjective (n=406)	Other (n=12)	Noun (n=1,262)	Verb (n=395)	Adjective (n=406)	Other (n=12)
mT5-Base	0.685	0.662	0.568	0.750	0.611	0.602	0.486	0.723
Qwen2.5-1.5B	0.743	0.725	0.715	0.775	0.721	0.700	0.687	0.711
Qwen2.5-1.5B-Instruct	0.740	0.722	0.715	0.766	0.722	0.698	0.687	0.704
Qwen2.5-7B	0.821	0.809	0.808	0.829	0.795	0.786	0.783	0.814
Qwen2.5-7B-Instruct	0.815	0.803	0.803	0.821	0.795	0.785	0.782	0.813
Goldfish German	0.720	0.747	0.701	0.769	0.758	0.772	0.742	0.769

Table 27: Breakdown of lemma classification accuracy by Part of Speech (POS) for each model, using Linear Regression and Multi-Layer Perceptron (MLP) classifiers (German). Lemmas are grouped by their POS tags (*e.g.*, , Noun, Verb, Adjective). Accuracies are calculated over all examples for a given group across all layers. Counts (n) are derived from a single representative layer for each group. All accuracy values are on a 0–1 scale.

Model	Base (n=688)	3rd person (n=776)	Positive (n=1,833)	Past (n=857)	Plural (n=1,457)	Singular (n=5,169)
mT5-Base	0.934	0.912	0.879	0.908	0.954	0.970
Qwen2.5-1.5B	0.933	0.858	0.896	0.903	0.958	0.967
Qwen2.5-1.5B-Instruct	0.930	0.852	0.893	0.898	0.958	0.966
Qwen2.5-7B	0.955	0.918	0.918	0.931	0.965	0.975
Qwen2.5-7B-Instruct	0.951	0.913	0.915	0.928	0.964	0.974
Goldfish French	0.942	0.955	0.937	0.930	0.968	0.976

Table 28: Breakdown of inflection classification accuracy for each model by inflection type using Linear Regression classifiers (French). Accuracies are calculated over all examples for a given group across all layers. Counts (n) are derived from a single representative layer for each group. All accuracy values are on a 0–1 scale.

Model	Base (n=688)	3rd person (n=776)	Positive (n=1,833)	Past (n=857)	Plural (n=1,457)	Singular (n=5,169)
mT5-Base	0.957	0.937	0.911	0.935	0.957	0.977
Qwen2.5-1.5B	0.954	0.905	0.914	0.925	0.965	0.968
Qwen2.5-1.5B-Instruct	0.954	0.902	0.911	0.924	0.965	0.968
Qwen2.5-7B	0.966	0.936	0.930	0.937	0.970	0.976
Qwen2.5-7B-Instruct	0.962	0.931	0.926	0.934	0.970	0.975
Goldfish French	0.974	0.967	0.945	0.942	0.973	0.979

Table 29: Breakdown of inflection classification accuracy for each model by inflection type using Multi-Layer Perceptron (MLP) classifiers (French). Accuracies are calculated over all examples for a given group across all layers. Counts (n) are derived from a single representative layer for each group. All accuracy values are on a 0–1 scale.

Model	Linear Regression				MLP			
	Noun (n=1,496)	Verb (n=406)	Adjective (n=358)	Other (n=15)	Noun (n=1,496)	Verb (n=406)	Adjective (n=358)	Other (n=15)
mT5-Base	0.708	0.577	0.605	0.799	0.755	0.560	0.636	0.820
Qwen2.5-1.5B	0.754	0.725	0.673	0.824	0.807	0.765	0.751	0.853
Qwen2.5-1.5B-Instruct	0.750	0.718	0.671	0.820	0.824	0.776	0.768	0.869
Qwen2.5-7B	0.840	0.814	0.764	0.869	0.856	0.825	0.794	0.884
Qwen2.5-7B-Instruct	0.833	0.805	0.758	0.860	0.851	0.818	0.792	0.883
Goldfish French	0.749	0.758	0.661	0.811	0.894	0.869	0.813	0.888

Table 30: Breakdown of lemma classification accuracy by Part of Speech (POS) for each model, using Linear Regression and Multi-Layer Perceptron (MLP) classifiers (French). Lemmas are grouped by their POS tags (*e.g.*, , Noun, Verb, Adjective). Accuracies are calculated over all examples for a given group across all layers. Counts (n) are derived from a single representative layer for each group. All accuracy values are on a 0–1 scale.

Model	Base (n=690)	3rd person (n=456)	Positive (n=1,192)	Past (n=455)	Plural (n=1,333)	Superlative (n=3)	Singular (n=3,316)	Comparative (n=23)
mT5-Base	0.930	0.978	0.975	0.957	0.877	0.000	0.977	0.799
Qwen2.5-1.5B	0.925	0.946	0.974	0.938	0.923	0.015	0.966	0.835
Qwen2.5-1.5B-Instruct	0.924	0.943	0.974	0.934	0.921	0.015	0.966	0.817
Qwen2.5-7B	0.949	0.966	0.979	0.958	0.948	0.094	0.977	0.872
Qwen2.5-7B-Instruct	0.951	0.974	0.980	0.970	0.948	0.080	0.980	0.918
Goldfish Russian	0.940	0.950	0.976	0.931	0.921	0.000	0.976	0.867

Table 31: Breakdown of inflection classification accuracy for each model by inflection type using Linear Regression classifiers (Russian). Accuracies are calculated over all examples for a given group across all layers. Counts (n) are derived from a single representative layer for each group. All accuracy values are on a 0–1 scale.

Model	Base (n=690)	3rd person (n=456)	Positive (n=1,192)	Past (n=455)	Plural (n=1,333)	Superlative (n=3)	Singular (n=3,316)	Comparative (n=23)
mT5-Base	0.959	0.978	0.969	0.966	0.904	0.000	0.978	0.849
Qwen2.5-1.5B	0.952	0.955	0.972	0.948	0.933	0.089	0.970	0.899
Qwen2.5-1.5B-Instruct	0.950	0.954	0.973	0.947	0.933	0.089	0.969	0.911
Qwen2.5-7B	0.963	0.964	0.978	0.960	0.951	0.246	0.979	0.910
Qwen2.5-7B-Instruct	0.961	0.970	0.978	0.966	0.949	0.126	0.980	0.924
Goldfish Russian	0.965	0.972	0.978	0.948	0.943	0.000	0.977	0.934

Table 32: Breakdown of inflection classification accuracy for each model by inflection type using Multi-Layer Perceptron (MLP) classifiers (Russian). Accuracies are calculated over all examples for a given group across all layers. Counts (n) are derived from a single representative layer for each group. All accuracy values are on a 0–1 scale.

Model	Linear Regression				MLP			
	Noun (n=982)	Verb (n=333)	Adjective (n=275)	Other (n=4)	Noun (n=982)	Verb (n=333)	Adjective (n=275)	Other (n=4)
mT5-Base	0.660	0.614	0.542	0.648	0.492	0.484	0.387	0.426
Qwen2.5-1.5B	0.777	0.712	0.759	0.720	0.712	0.696	0.716	0.647
Qwen2.5-1.5B-Instruct	0.772	0.704	0.756	0.720	0.710	0.689	0.717	0.643
Qwen2.5-7B	0.854	0.790	0.843	0.812	0.798	0.794	0.813	0.749
Qwen2.5-7B-Instruct	0.845	0.778	0.835	0.807	0.794	0.785	0.809	0.744
Goldfish Russian	0.795	0.723	0.764	0.676	0.810	0.776	0.759	0.657

Table 33: Breakdown of lemma classification accuracy by Part of Speech (POS) for each model, using Linear Regression and Multi-Layer Perceptron (MLP) classifiers (Russian). Lemmas are grouped by their POS tags (*e.g.*, , Noun, Verb, Adjective). Accuracies are calculated over all examples for a given group across all layers. Counts (n) are derived from a single representative layer for each group. All accuracy values are on a 0–1 scale.

Model	Base (n=154)	3rd person (n=51)	Positive (n=401)	Past (n=168)	Plural (n=33)	Singular (n=632)
mT5-Base	0.860	0.911	0.928	0.966	0.837	0.952
Qwen2.5-1.5B	0.808	0.802	0.721	0.928	0.861	0.892
Qwen2.5-1.5B-Instruct	0.809	0.817	0.720	0.941	0.878	0.899
Qwen2.5-7B	0.865	0.879	0.810	0.966	0.903	0.909
Qwen2.5-7B-Instruct	0.850	0.874	0.796	0.960	0.886	0.900
Goldfish Turkish	0.847	0.915	0.880	0.964	0.872	0.963

Table 34: Breakdown of inflection classification accuracy for each model by inflection type using Linear Regression classifiers (Turkish). Accuracies are calculated over all examples for a given group across all layers. Counts (n) are derived from a single representative layer for each group. All accuracy values are on a 0–1 scale.

Model	Base (n=154)	3rd person (n=51)	Positive (n=401)	Past (n=168)	Plural (n=33)	Singular (n=632)
mT5-Base	0.755	0.760	0.848	0.922	0.515	0.949
Qwen2.5-1.5B	0.770	0.767	0.667	0.919	0.765	0.914
Qwen2.5-1.5B-Instruct	0.762	0.757	0.662	0.917	0.766	0.913
Qwen2.5-7B	0.853	0.845	0.791	0.956	0.875	0.937
Qwen2.5-7B-Instruct	0.845	0.844	0.786	0.956	0.875	0.932
Goldfish Turkish	0.832	0.879	0.870	0.957	0.834	0.957

Table 35: Breakdown of inflection classification accuracy for each model by inflection type using Multi-Layer Perceptron (MLP) classifiers (Turkish). Accuracies are calculated over all examples for a given group across all layers. Counts (n) are derived from a single representative layer for each group. All accuracy values are on a 0–1 scale.

Model	Linear Regression				MLP			
	Noun (n=221)	Verb (n=53)	Adjective (n=104)	Other (n=13)	Noun (n=221)	Verb (n=53)	Adjective (n=104)	Other (n=13)
mT5-Base	0.866	0.823	0.921	0.955	0.215	0.421	0.374	0.637
Qwen2.5-1.5B	0.834	0.805	0.866	0.877	0.307	0.439	0.449	0.693
Qwen2.5-1.5B-Instruct	0.816	0.791	0.860	0.874	0.305	0.439	0.448	0.691
Qwen2.5-7B	0.871	0.850	0.900	0.904	0.595	0.625	0.695	0.809
Qwen2.5-7B-Instruct	0.850	0.823	0.883	0.885	0.579	0.613	0.678	0.800
Goldfish Turkish	0.929	0.904	0.940	0.969	0.386	0.550	0.477	0.808

Table 36: Breakdown of lemma classification accuracy by Part of Speech (POS) for each model, using Linear Regression and Multi-Layer Perceptron (MLP) classifiers (Turkish). Lemmas are grouped by their POS tags (*e.g.*, , Noun, Verb, Adjective). Accuracies are calculated over all examples for a given group across all layers. Counts (n) are derived from a single representative layer for each group. All accuracy values are on a 0–1 scale.